

B

Mesozoic Stratigraphy



Mutti et al 2009 Sedimentology v 56 pp 267-318

U C Monte Cassio Flysch, Baganza valley, Northern Apennines



Pre-Alpine Orogeny or (a in map) not involved in orogens

Limestones and marly limestones with chert, radiolarites, calcareous marls, marls and pelites, locally interbedded turbiditic calcarenites (34); idem, frequently interbedded with calcarenitic and arenaceous turbidites, locally condensed limestones and marls (35)
 Cretaceous-Tortonian, locally up to Pliocene

Shales and radiolarites, with alternating marls and turbiditic calcarenites (36); idem, with low- to very low-grade metamorphism (37)
 Cretaceous-Lower Miocene, locally since Middle Jurassic

Limestones and dolostones with chert, radiolarites and marls; conglomerates, sandstones, pelites; slates and cherty slates (38); idem, with low- to very low-grade metamorphism (39); Limestones and dolostones with chert, radiolarites and marls, frequently interbedded turbiditic calcarenites (40)
 Jurassic-Lower Cretaceous, locally since Upper Triassic

Nodular limestones, sometimes dolomitized, and nodular marls
 Jurassic, since Pliensbachian

Limestones and dolostones, sometimes cherty, marly limestones and pelites, locally bituminous, with calcarenitic intercalations
 Middle Triassic-Lower Jurassic

Limestones, dolostones, pelites and sandstones, with frequent intercalations of turbiditic calcarenites and basalts
 Permian

Symbols

Dashed where inferred or buried

Edge of caldera

Undifferentiated tectonic contact

Normal fault

Strike-slip fault

Thrust and reverse fault

Epi-oceanic and epi-continental Platform and proximal Ramp carbonate deposits

Pre-Alpine Orogeny or (a in map) not involved in orogens

Organogenic and detrital limestones, locally sandstones
 Miocene-Lower Pleistocene, locally since Oligocene

Limestones, dolomitic limestones and dolostones, locally with bauxites in the lower part
 Upper Cretaceous, locally since Lower Cretaceous or up to Paleogene

Limestones, dolomitic limestones and dolostones
 Middle Jurassic-Paleogene

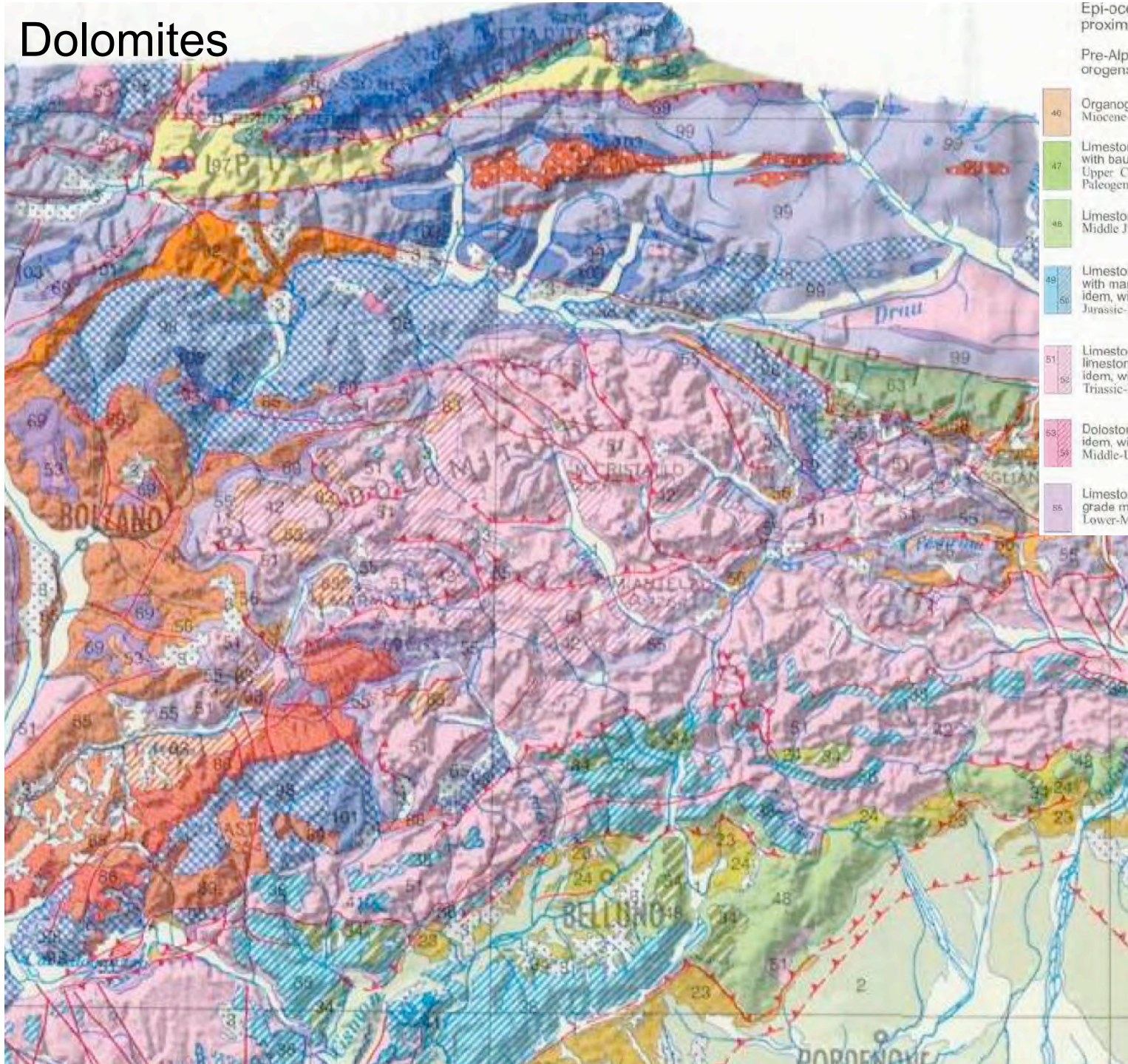
Limestones, dolomitic limestones and dolostones, locally with marly levels (49); idem, with low- to very low-grade metamorphism (50)
 Jurassic-Lower Cretaceous

Limestones, dolomitic limestones and dolostones; marly limestones, marls and bituminous shales (51); idem, with low- to very low-grade metamorphism (52)
 Triassic-Lower Jurassic

Dolostones, marls and evaporites (53); idem, with low- to very low-grade metamorphism (54)
 Middle-Upper Triassic, locally up to Lower Jurassic

Limestones, sandstones and pelites, locally with low-grade metamorphism
 Lower-Middle Triassic

Dolomites



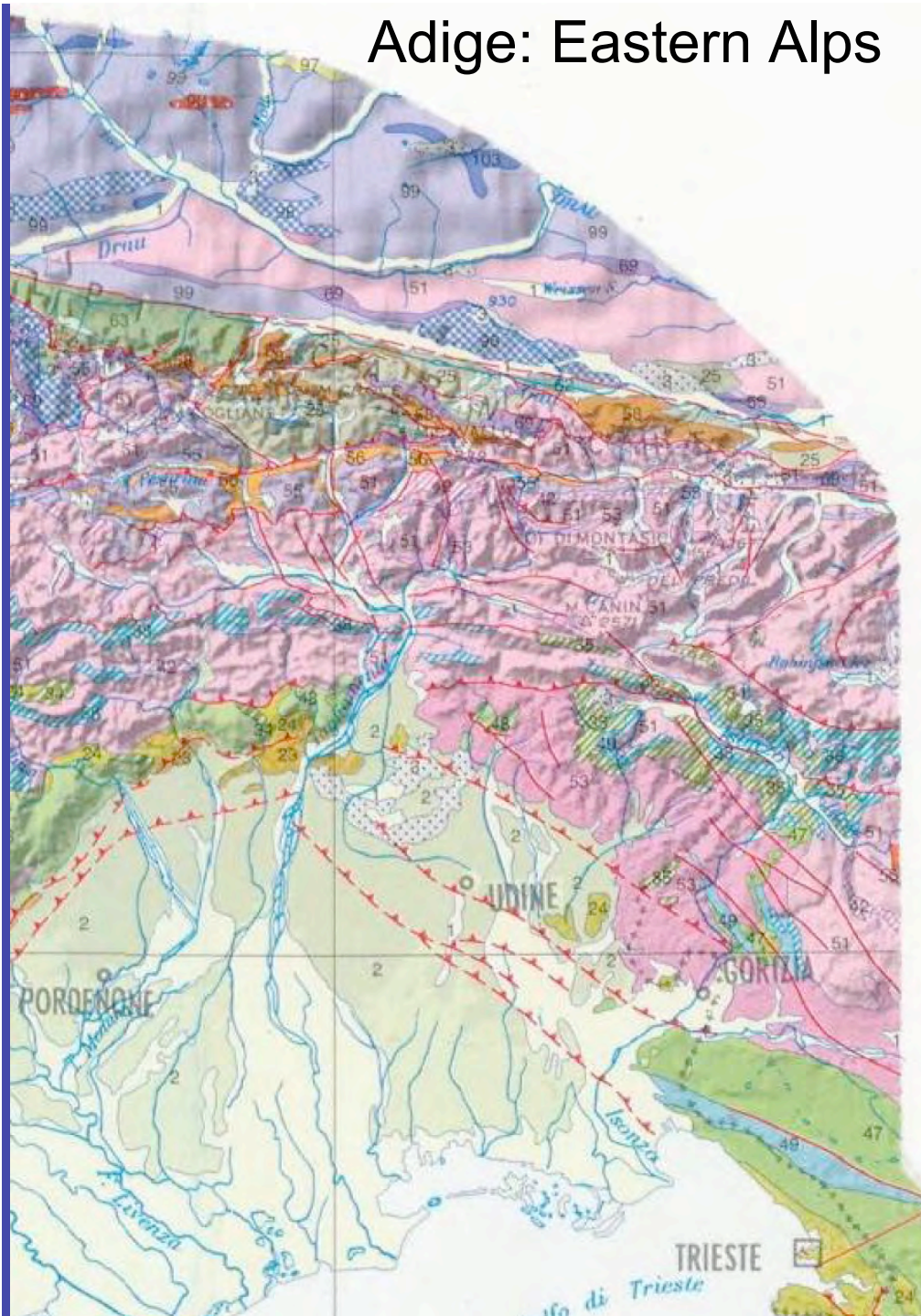
Epi-oceanic and epi-continental Platform and proximal Ramp carbonate deposits

Pre-Alpine Orogeny or (a in map) not involved in orogens

- 46 Organogenic and detrital limestones, locally sandstones
Miocene-Lower Pleistocene, locally since Oligocene
- 47 Limestones, dolomitic limestones and dolostones, locally with bauxites in the lower part
Upper Cretaceous, locally since Lower Cretaceous or up to Paleogene
- 48 Limestones, dolomitic limestones and dolostones
Middle Jurassic-Paleogene
- 49 Limestones, dolomitic limestones and dolostones, locally with marly levels (49);
idem, with low- to very low-grade metamorphism (50)
Jurassic-Lower Cretaceous
- 51 Limestones, dolomitic limestones and dolostones; marly limestones, marls and bituminous shales (51);
idem, with low- to very low-grade metamorphism (52)
Triassic-Lower Jurassic
- 53 Dolostones, marls and evaporites (53);
idem, with low- to very low-grade metamorphism (54)
Middle-Upper Triassic, locally up to Lower Jurassic
- 55 Limestones, sandstones and pelitas, locally with low-grade metamorphism
Lower-Middle Triassic



Adige: Eastern Alps



Pre-Alpine Orogeny or (a in map) not involved in orogens

Limestones and marly limestones with chert, radiolarites, calcareous marls, marls and pelites, locally interbedded turbiditic calcarenites (34); idem, frequently interbedded with calcarenitic and arenaceous turbidites, locally condensed limestones and marls (35)
Cretaceous-Tortonian, locally up to Pliocene

Shales and radiolarites, with alternating marls and turbiditic calcarenites (36); idem, with low- to very low-grade metamorphism (37)
Cretaceous-Lower Miocene, locally since Middle Jurassic

Limestones and dolostones with chert, radiolarites and marls; conglomerates, sandstones, pelites; slates and cherty slates (38); idem, with low- to very low-grade metamorphism (39); Limestones and dolostones with chert, radiolarites and marls, frequently interbedded turbiditic calcarenites (40)
Jurassic-Lower Cretaceous, locally since Upper Triassic

Nodular limestones, sometimes dolomitized, and nodular marls
Jurassic, since Pliensbachian

Limestones and dolostones, sometimes cherty, marly limestones and pelites, locally bituminous, with calcarenitic intercalations
Middle Triassic-Lower Jurassic

Limestones, dolostones, pelites and sandstones, with frequent intercalations of turbiditic calcarenites and basalts
Permian

Epi-oceanic and epi-continental Platform and proximal Ramp carbonate deposits

Pre-Alpine Orogeny or (a in map) not involved in orogens

Organogenic and detrital limestones, locally sandstones
Miocene-Lower Pleistocene, locally since Oligocene

Limestones, dolomitic limestones and dolostones, locally with bauxites in the lower part
Upper Cretaceous, locally since Lower Cretaceous or up to Paleogene

Limestones, dolomitic limestones and dolostones
Middle Jurassic-Paleogene

Limestones, dolomitic limestones and dolostones, locally with marly levels (49); idem, with low- to very low-grade metamorphism (50)
Jurassic-Lower Cretaceous

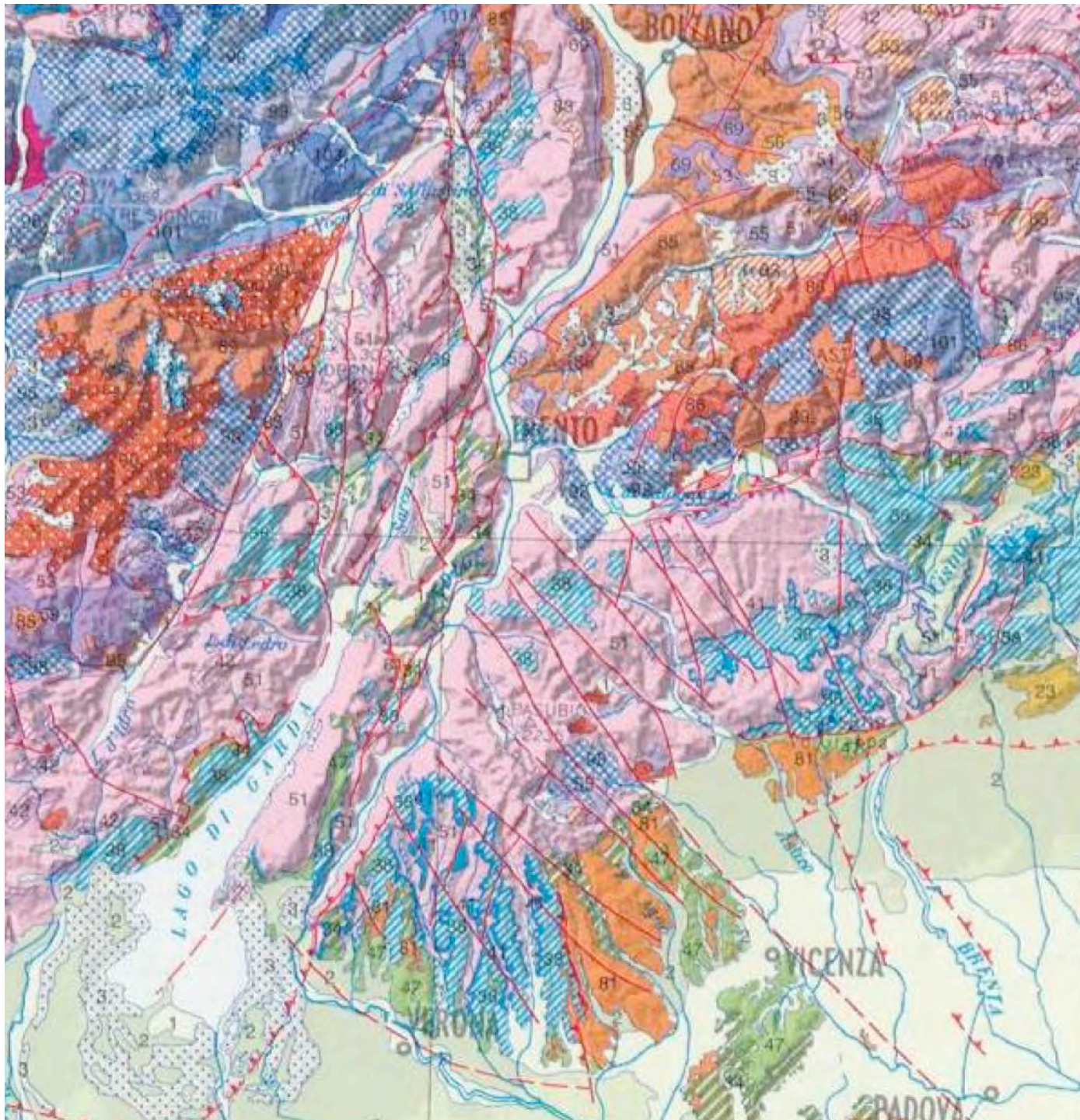
Limestones, dolomitic limestones and dolostones; marly limestones, marls and bituminous shales (51); idem, with low- to very low-grade metamorphism (52)
Triassic-Lower Jurassic

Dolostones, marls and evaporites (53); idem, with low- to very low-grade metamorphism (54)
Middle-Upper Triassic, locally up to Lower Jurassic

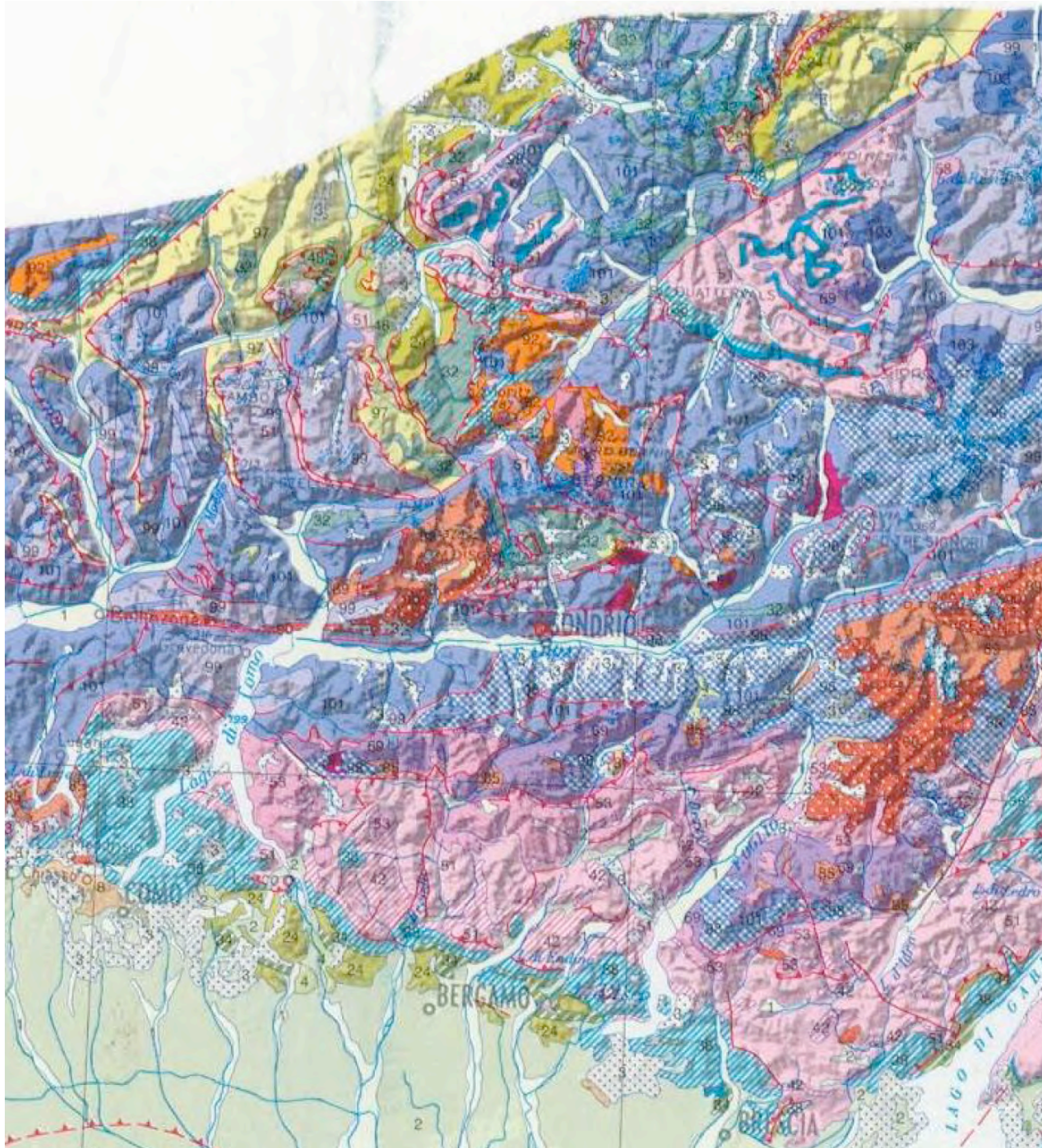
Limestones, sandstones and pelites, locally with low-grade metamorphism
Lower-Middle Triassic

Symbols

- Dashed where inferred or buried
- Edge of caldera
- Undifferentiated tectonic contact
- Normal fault
- Strike-slip fault
- Thrust and reverse fault



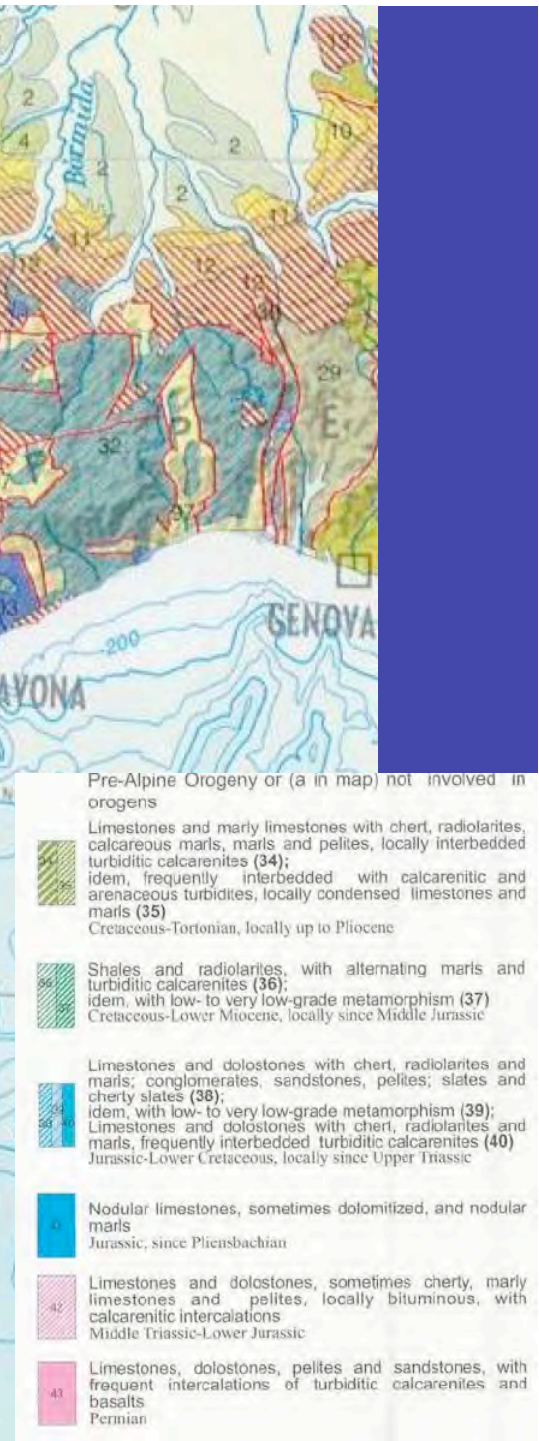
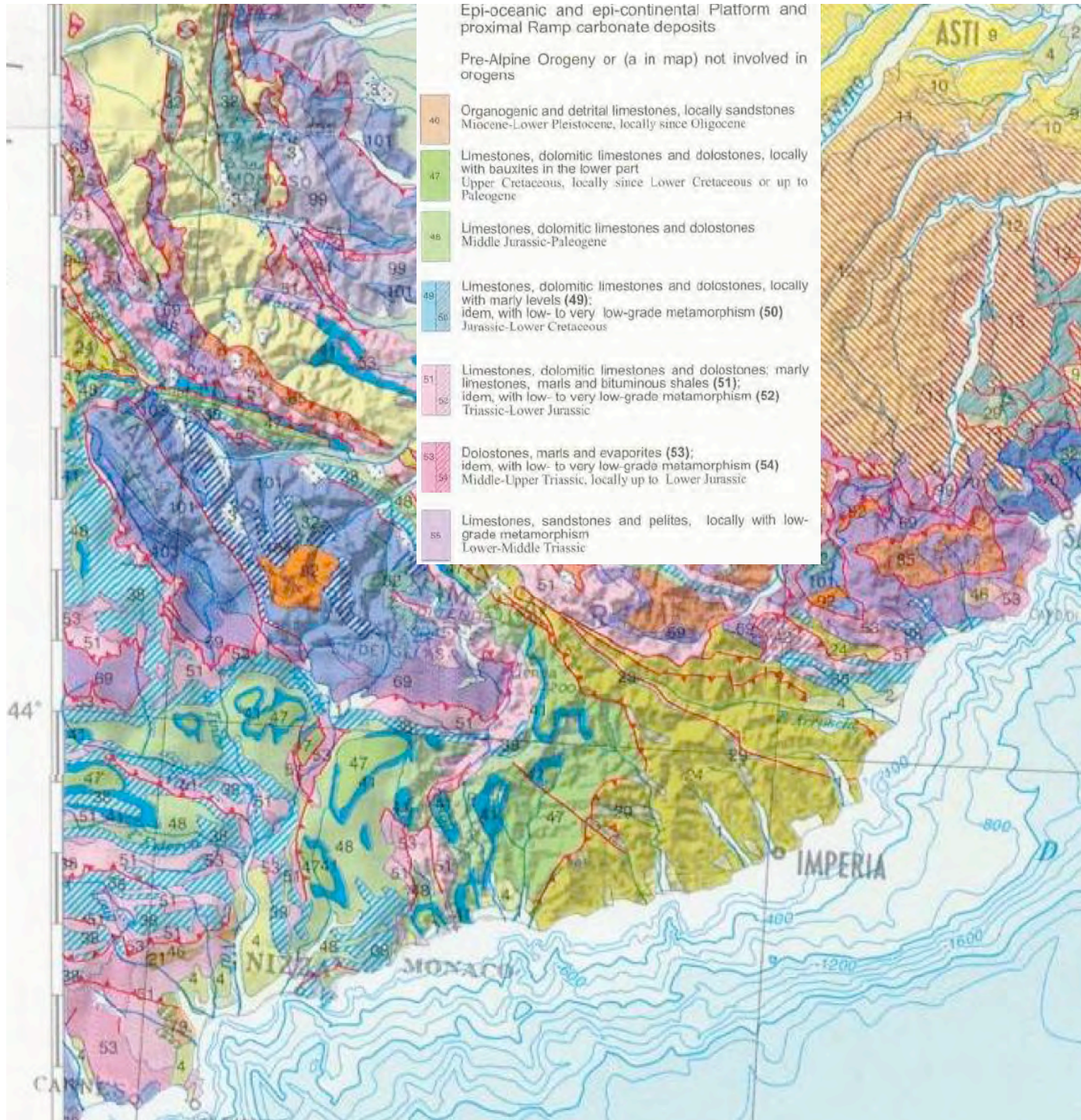
- Pre-Alpine Orogeny or (a in map) not involved in orogens
 - Limestones and marly limestones with chert, radiolarites, calcareous marls, marls and pelites, locally interbedded turbiditic calcarenites (34); idem, frequently interbedded with calcarenitic and arenaceous turbidites, locally condensed limestones and marls (35)
Cretaceous-Tortonian, locally up to Pliocene
 - Shales and radiolarites, with alternating marls and turbiditic calcarenites (36); idem, with low- to very low-grade metamorphism (37)
Cretaceous-Lower Miocene, locally since Middle Jurassic
 - Limestones and dolostones with chert, radiolarites and marls; conglomerates, sandstones, pelites; slates and cherty slates (38); idem, with low- to very low-grade metamorphism (39); Limestones and dolostones with chert, radiolarites and marls, frequently interbedded turbiditic calcarenites (40)
Jurassic-Lower Cretaceous, locally since Upper Triassic
 - Nodular limestones, sometimes dolomitized, and nodular marls
Jurassic, since Pliensbachian
 - Limestones and dolostones, sometimes cherty, marly limestones and pelites, locally bituminous, with calcarenitic intercalations
Middle Triassic-Lower Jurassic
 - Limestones, dolostones, pelites and sandstones, with frequent intercalations of turbiditic calcarenites and basalts
Permian
-
- Epi-oceanic and epi-continental Platform and proximal Ramp carbonate deposits
 - Pre-Alpine Orogeny or (a in map) not involved in orogens
 - Organogenic and detrital limestones, locally sandstones
Miocene-Lower Pleistocene, locally since Oligocene
 - Limestones, dolomitic limestones and dolostones, locally with bauxites in the lower part
Upper Cretaceous, locally since Lower Cretaceous or up to Paleogene
 - Limestones, dolomitic limestones and dolostones
Middle Jurassic-Paleogene
 - Limestones, dolomitic limestones and dolostones, locally with marly levels (49); idem, with low- to very low-grade metamorphism (50)
Jurassic-Lower Cretaceous
 - Limestones, dolomitic limestones and dolostones; marly limestones, marls and bituminous shales (51); idem, with low- to very low-grade metamorphism (52)
Triassic-Lower Jurassic
 - Dolostones, marls and evaporites (53); idem, with low- to very low-grade metamorphism (54)
Middle-Upper Triassic, locally up to Lower Jurassic
 - Limestones, sandstones and pelites, locally with low-grade metamorphism
Lower-Middle Triassic



- Pre-Alpine Orogeny or (a in map) not involved in orogens
- Limestones and marly limestones with chert, radiolarites, calcareous marls, marls and pelites, locally interbedded turbiditic calcarenites (34); idem, frequently interbedded with calcarenitic and arenaceous turbidites, locally condensed limestones and marls (35)
 Cretaceous-Tortonian, locally up to Pliocene
- Shales and radiolarites, with alternating marls and turbiditic calcarenites (36); idem, with low- to very low-grade metamorphism (37)
 Cretaceous-Lower Miocene, locally since Middle Jurassic
- Limestones and dolostones with chert, radiolarites and marls; conglomerates, sandstones, pelites; slates and cherty slates (38); idem, with low- to very low-grade metamorphism (39); Limestones and dolostones with chert, radiolarites and marls, frequently interbedded turbiditic calcarenites (40)
 Jurassic-Lower Cretaceous, locally since Upper Triassic
- Nodular limestones, sometimes dolomitized, and nodular marls
 Jurassic, since Pliensbachian
- Limestones and dolostones, sometimes cherty, marly limestones and pelites, locally bituminous, with calcarenitic intercalations
 Middle Triassic-Lower Jurassic
- Limestones, dolostones, pelites and sandstones, with frequent intercalations of turbiditic calcarenites and basalts
 Permian

- Epi-oceanic and epi-continental Platform and proximal Ramp carbonate deposits

 Pre-Alpine Orogeny or (a in map) not involved in orogens
- Organogenic and detrital limestones, locally sandstones
 Miocene-Lower Pleistocene, locally since Oligocene
- Limestones, dolomitic limestones and dolostones, locally with bauxites in the lower part
 Upper Cretaceous, locally since Lower Cretaceous or up to Paleogene
- Limestones, dolomitic limestones and dolostones
 Middle Jurassic-Paleogene
- Limestones, dolomitic limestones and dolostones, locally with marly levels (49); idem, with low- to very low-grade metamorphism (50)
 Jurassic-Lower Cretaceous
- Limestones, dolomitic limestones and dolostones; marly limestones, marls and bituminous shales (51); idem, with low- to very low-grade metamorphism (52)
 Triassic-Lower Jurassic
- Dolostones, marls and evaporites (53); idem, with low- to very low-grade metamorphism (54)
 Middle-Upper Triassic, locally up to Lower Jurassic
- Limestones, sandstones and pelites, locally with low-grade metamorphism
 Lower-Middle Triassic



Gargano Peninsula



Data SIO, NOAA, U.S. Navy, NGA, GEBCO
© 2012 Cnes/Spot Image
Image © 2012 GeoEye
Image © 2012 DigitalGlobe

©2010 Google

Imagery Date: Jan 25, 2006

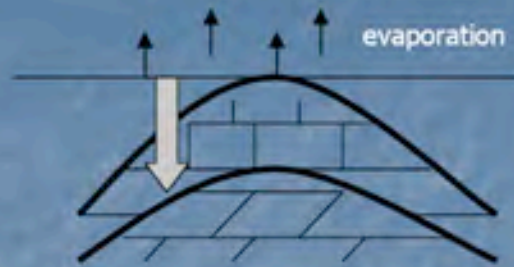
41°48'33.29" N 15°55'56.19" E elev 2341 ft

Eye alt 23.96 mi

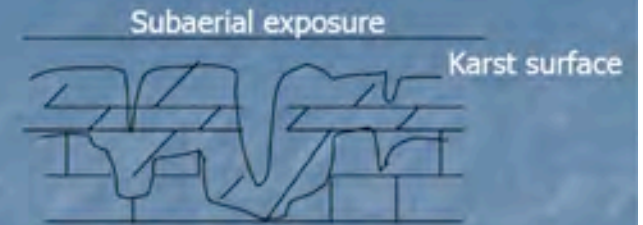
Near surface



Sabkha dolomites, Andrichuck (1960). Other model suggests reflux mechanism (Martindale et al, 2004)



Mound shape dolomite bodies formed by slightly evaporated seawater, Saller and Yaremko (1994)

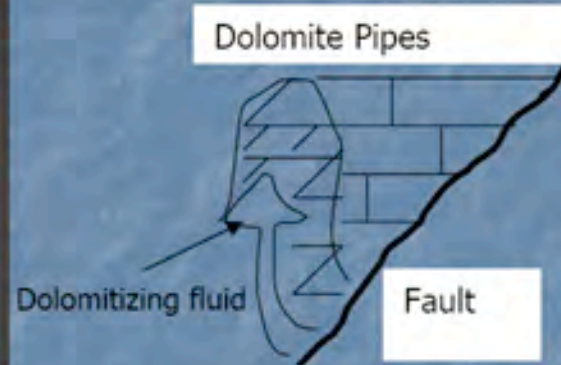


Karst porosity by subaerial exposure, Workum (1991)

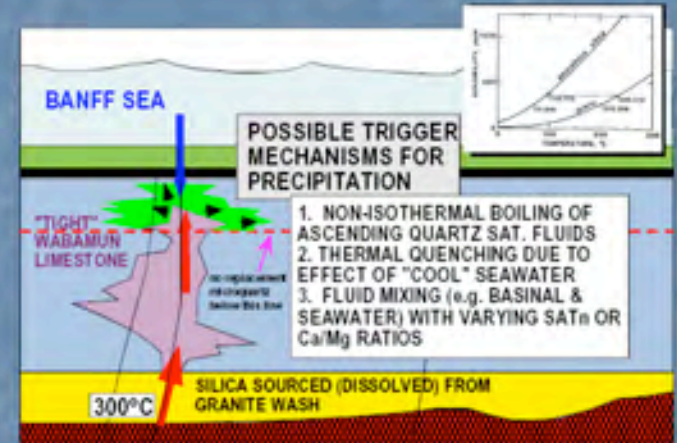
Subsurface



Fracture Associated Hydrothermal Karst (FAHK), Packard and Pellegrin (1990); Packard et al. (1990); Packard (1992)



Dolomite Pipes after fault associated hydrothermal fluid flow, Majid (1989).



Diffusely chertified dolostone bodies in the limestone-dolostone interface, Packard et al. (2001)

Models of dolomite alteration of limestone



Dolomite

<http://geology.com/minerals/dolomite.shtml>

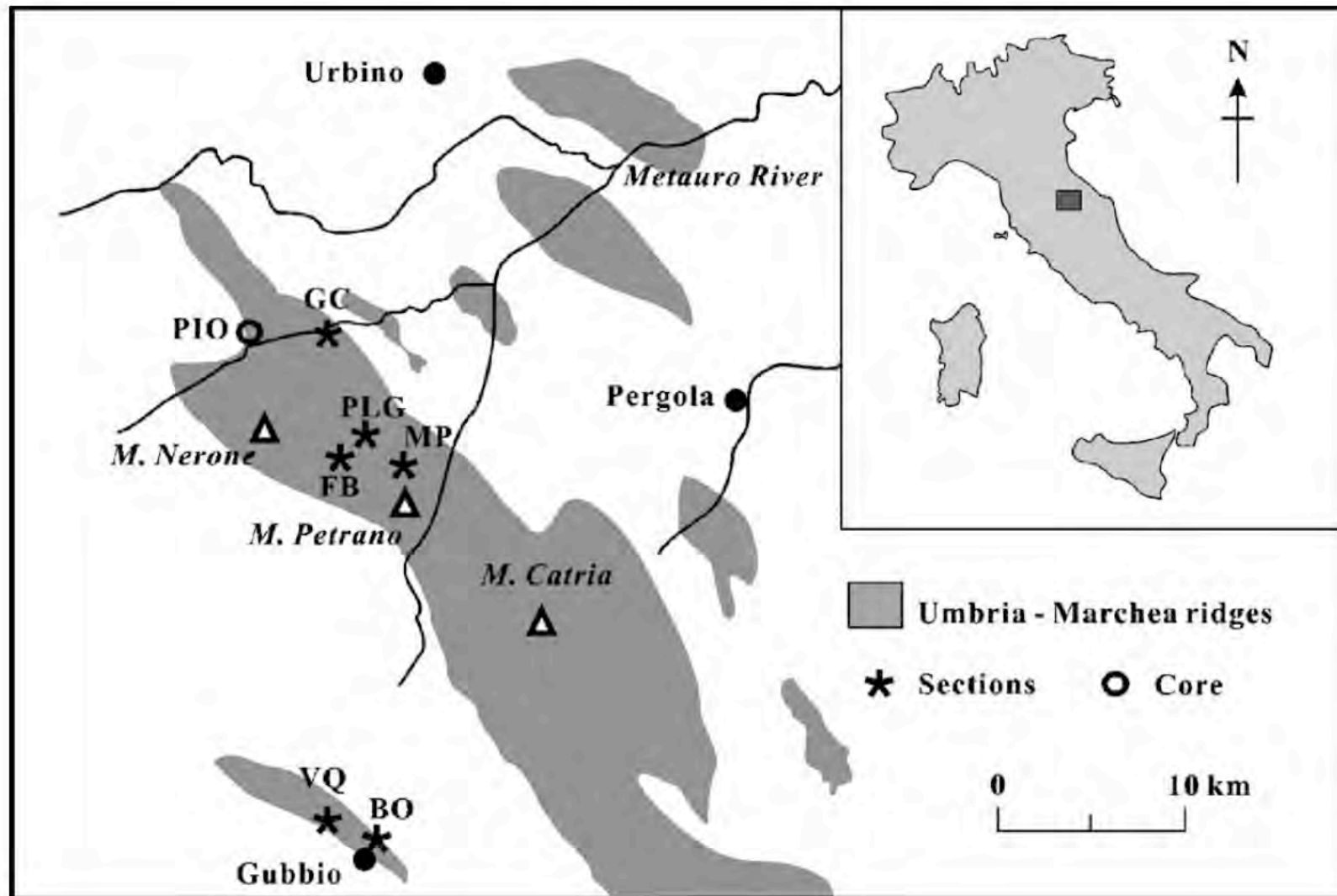
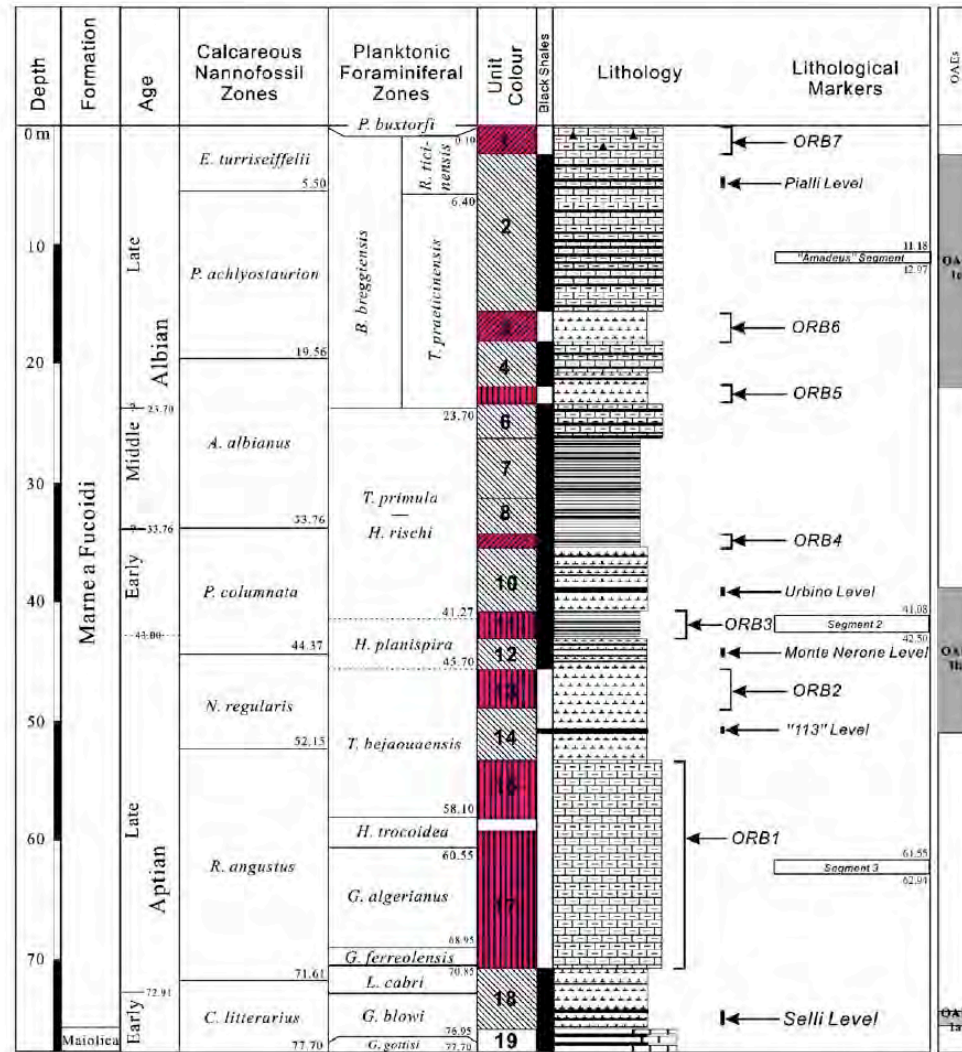


Fig. 1. Location of the studied sections near Gubbio–Piobbico area, the Umbria–Marche Basin, central Italy (modified from Baudin et al., 1998). Sections: BO: Bottaccione Gorge section; CQ: Vispi Quarry section; FB: Fiume Bosso section, GC: Gorgo a Cerbara section; MP: Monte Petrano section; PIO: Piobbico core; PLG: Poggio le Guaine section.



Piobbico Core

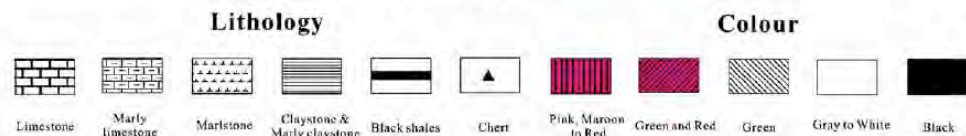


Fig. 2. Synthesis of stratigraphic data for the Piobbico core. Lithostratigraphy and integrated calcareous nannofossil-planktonic foraminiferal biostratigraphy are after Erba (1988), Tomaghi et al. (1989) and Erba (1992). Distinctive regional black shale levels, OAEs, and ORBs are marked in the right column. In the middle column, a more detailed color characteristic of the strata is presented. Also shown are locations of additional, perhaps more local OAEs, e.g., "113" Level, "Monte Nerone" Level, "Urbino" Level and "Pialli" Level (Cocconi et al., 1987, 1989, 1990; Cocconi and Galeotti, 1993; Cocconi, 2001; Galeotti et al., 2003).

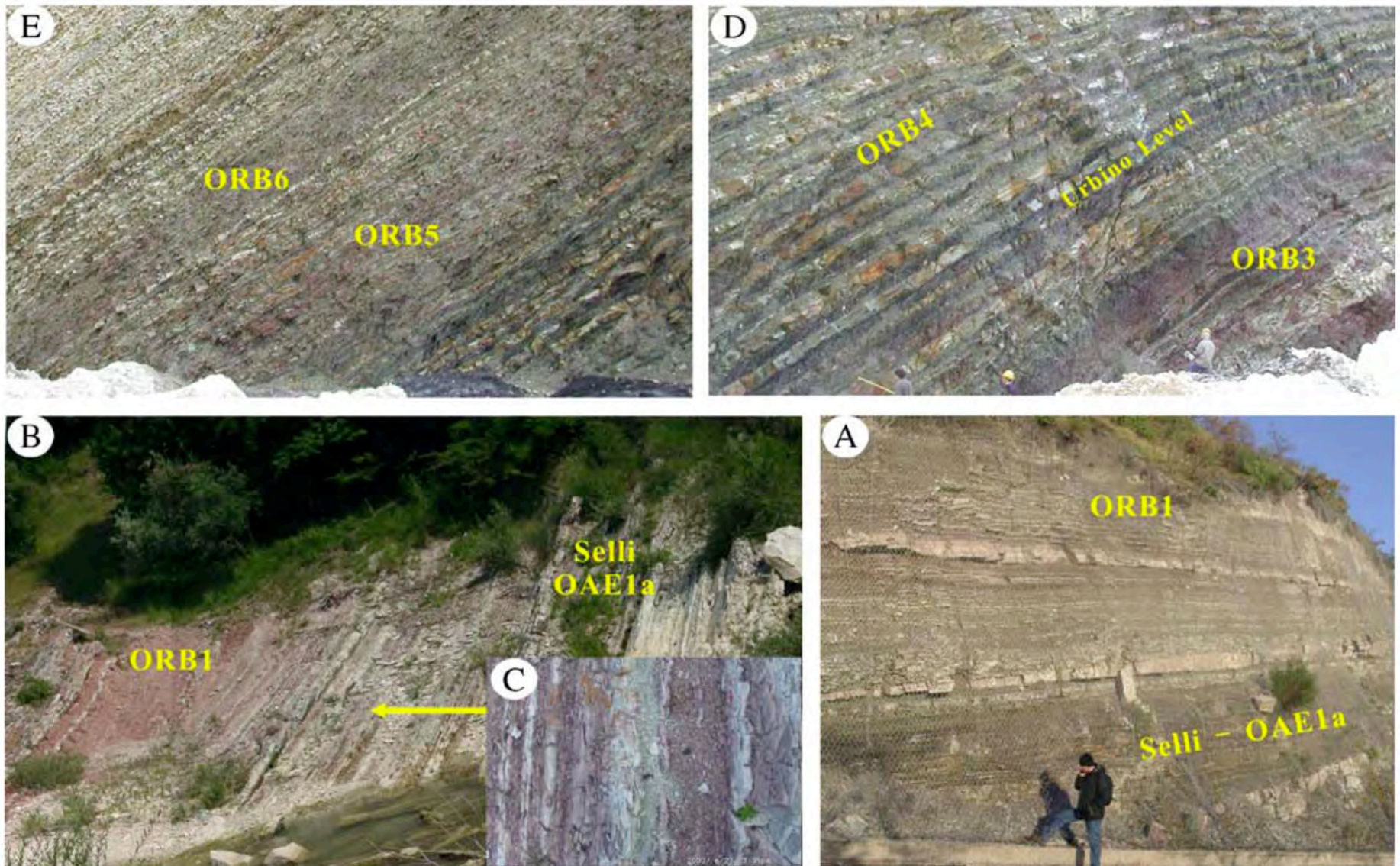
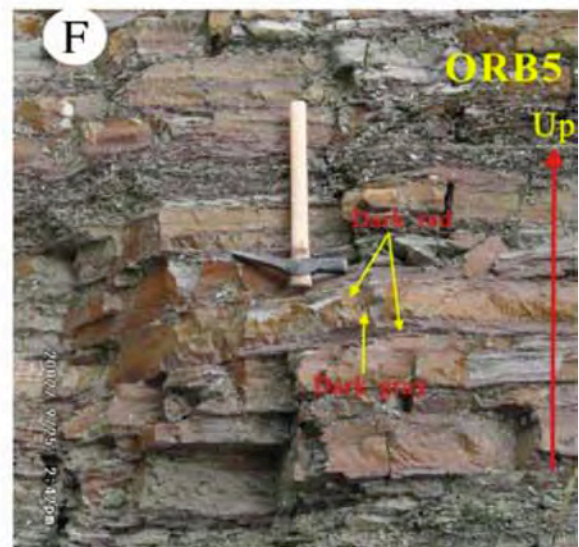
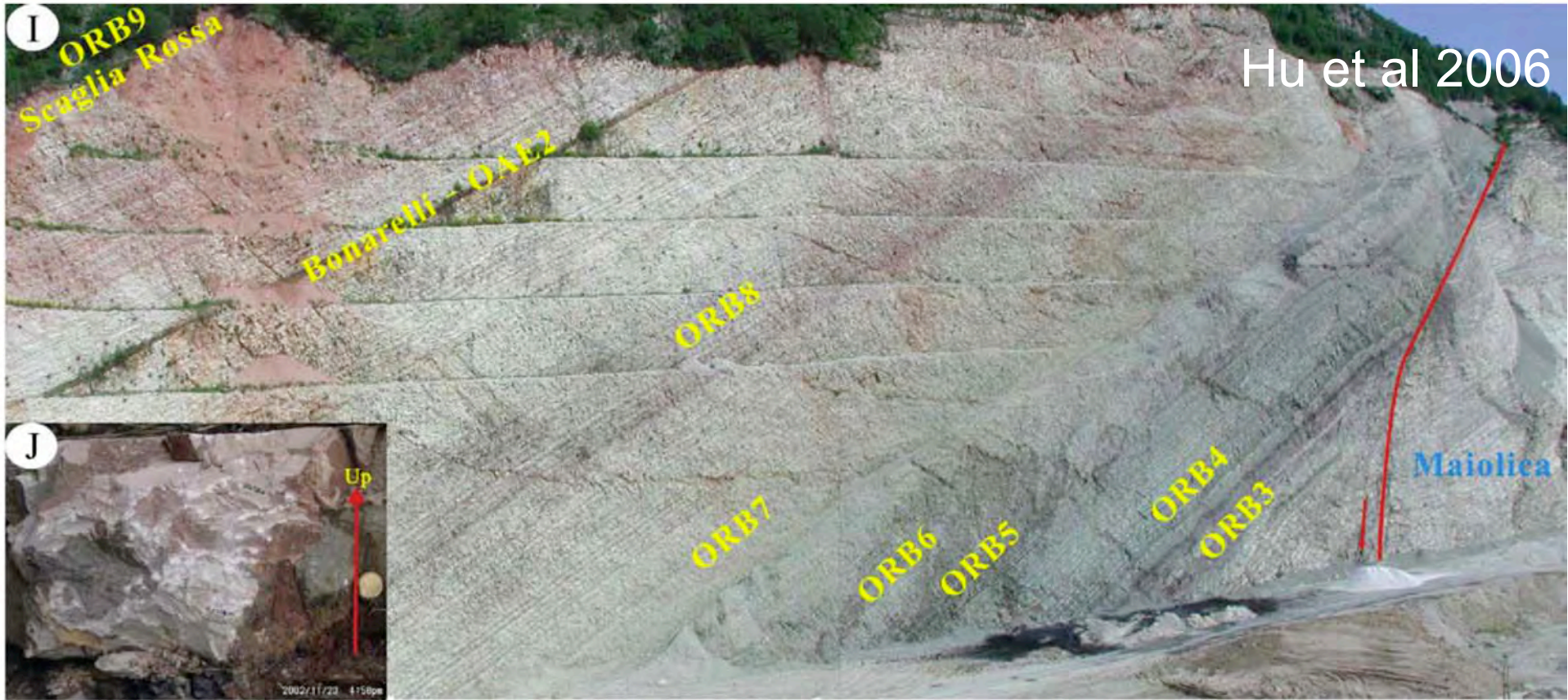


Fig. 3. Photographs showing the mid-Cretaceous ORBs in the Umbria–Marche Basin. (A–C) the early Aptian sequence, showing the change from early Aptian OAE1a–Selli Level to the first red bed–ORB1, in the Piobbico Road section (A) and in the Gorgo a Cerbara section (B). In the ORB1, the gray beds are interbedded with the red beds in a cyclic manner (B and C). The contacts between red beds and gray beds are usually sharp (C); (D) early Albian sequence showing the positions of the ORB3, ORB4, and the Urbino level in Vispi Quarry section; (E) late Albian sequence showing the positions of the ORB5 and ORB6 in the Vispi Quarry section; (F) close-up photo of the ORB5 in the Vispi Quarry section, showing millimeter-thick dark red horizons occurring near the top and bottom of the white-gray marly limestones; (G) close-up photo of the ORB6 in the Vispi Quarry section; (H) close-up photo of the ORB8 in the Vispi Quarry section showing that in some beds, a white color occurs at the bottom and gradually becomes into pinkish or dark reddish towards the top; (I) panoramic photo of the Vispi Quarry section showing the positions of the ORBs (from ORB3 to ORB9) and the Bonarelli level; (J) close-up photo of the transitional bed from Scaglia Bianca to Scaglia Rossa, which is whitish in color at the bottom and gradually becomes pinkish towards the top.



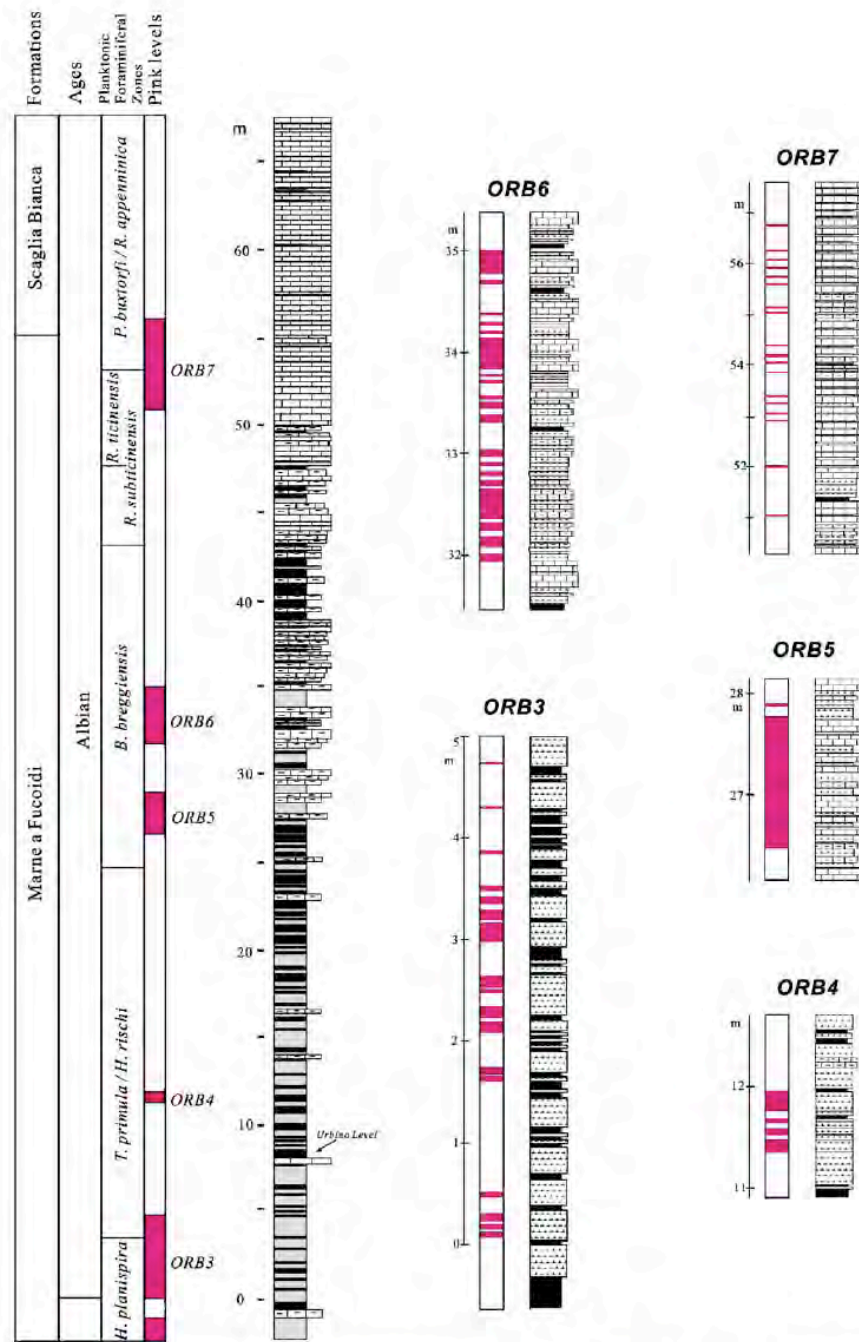


Fig. 4. The detailed lithostratigraphy and biostratigraphy of the Albian part of the Monte Petrano section. On the left side, the detailed lithology of the Albian strata and positions of ORBs are indicated; on the right side, lithology and color variation of five ORBs in the Albian section of the Monte Petrano are shown in more detail (modified after Fiet and Masure, 2001). Legend as in Fig. 2.

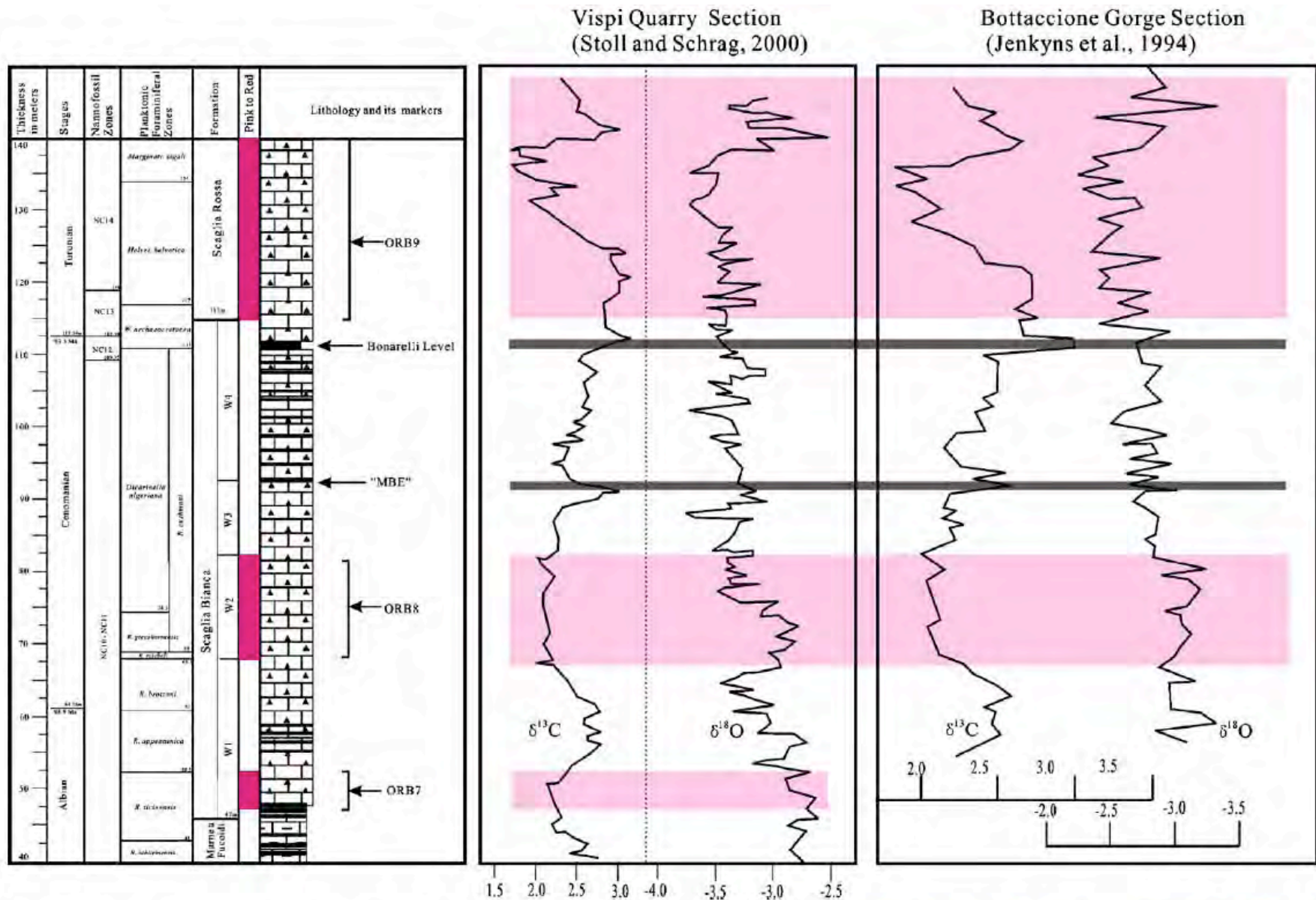


Fig. 5. Lithostratigraphy and biostratigraphy of the Albian–Turonian segment of the Bottaccione Gorge section (revised after Premoli Silva and Sliter, 1994; Tremolada, 2002; Coccioni and Galeotti, 2003) are shown plotted against the late Albian–late Turonian carbon and oxygen isotope record from the Bottaccione Gorge (Jenkyns et al., 1994) and Vispi Quarry (Stoll and Schrag, 2000). Note that the MCE (mid-Cenomanian event) and the Bonarelli event are associated with positive excursions of $\delta^{13}\text{C}$, while ORB7 and ORB8 correspond to low values on the carbon isotopes curve. Turned on in Fig. 2

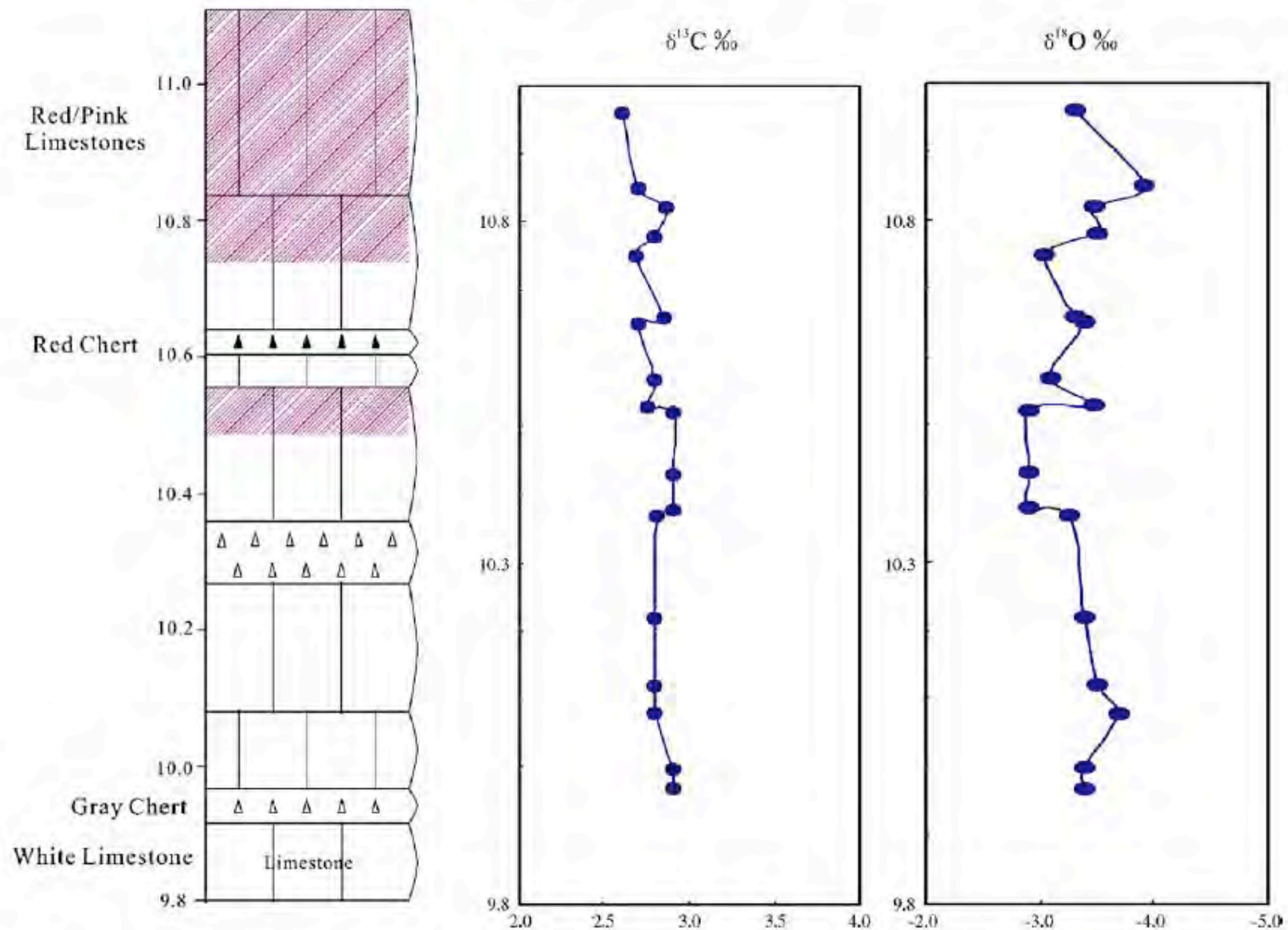


Fig. 6. Carbon and oxygen isotope records from the transition from Scaglia Bianca to Scaglia Rossa in the Vispi Quarry section. Note that there is no obvious isotopic change for the occurrences of the red beds.

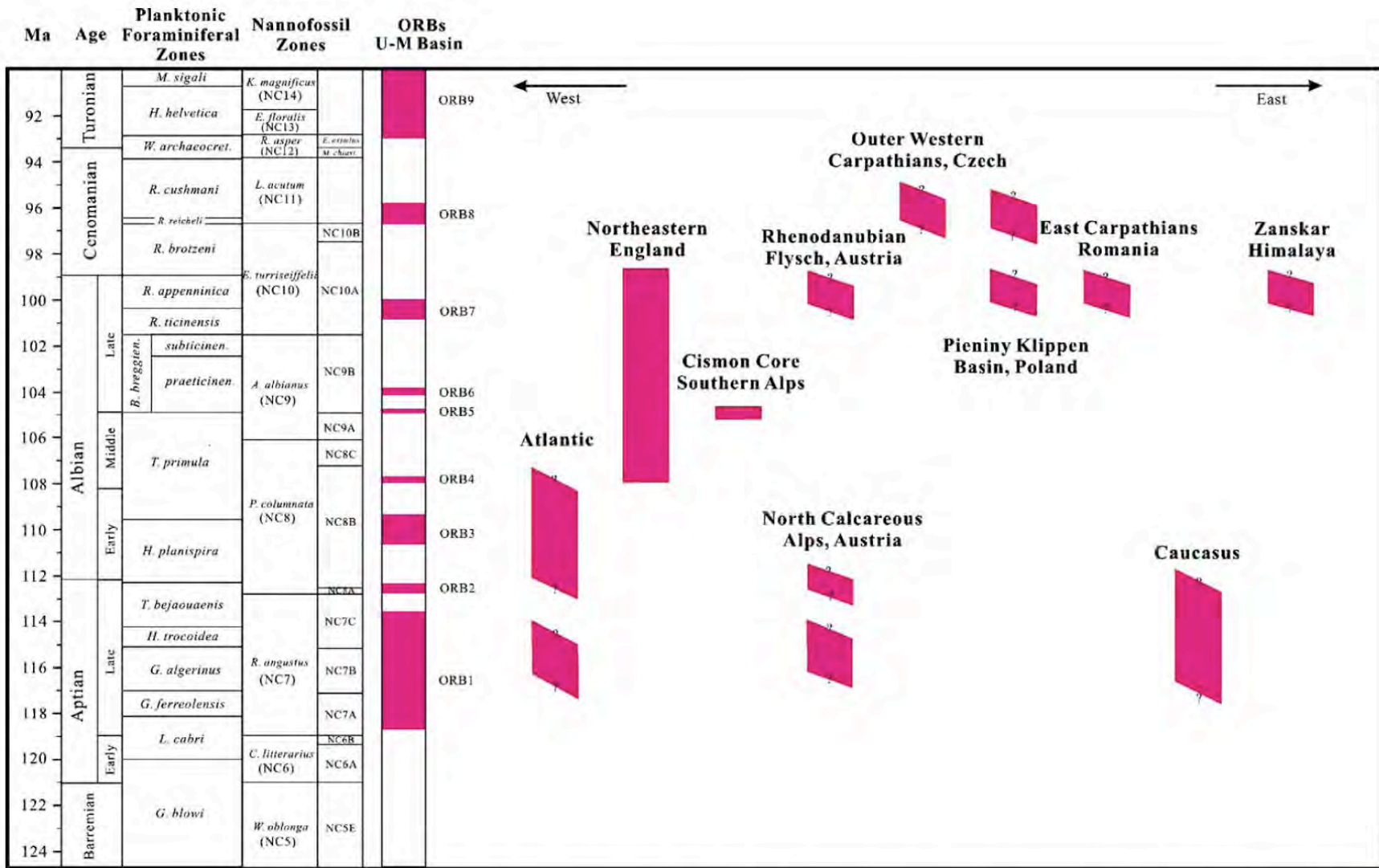


Fig. 8. Chronostratigraphic distributions of the mid-Cretaceous oceanic red beds in Tethys and Atlantic. The mid-Cretaceous integrated calcareous plankton biostratigraphy is after Leckie et al. (2002).

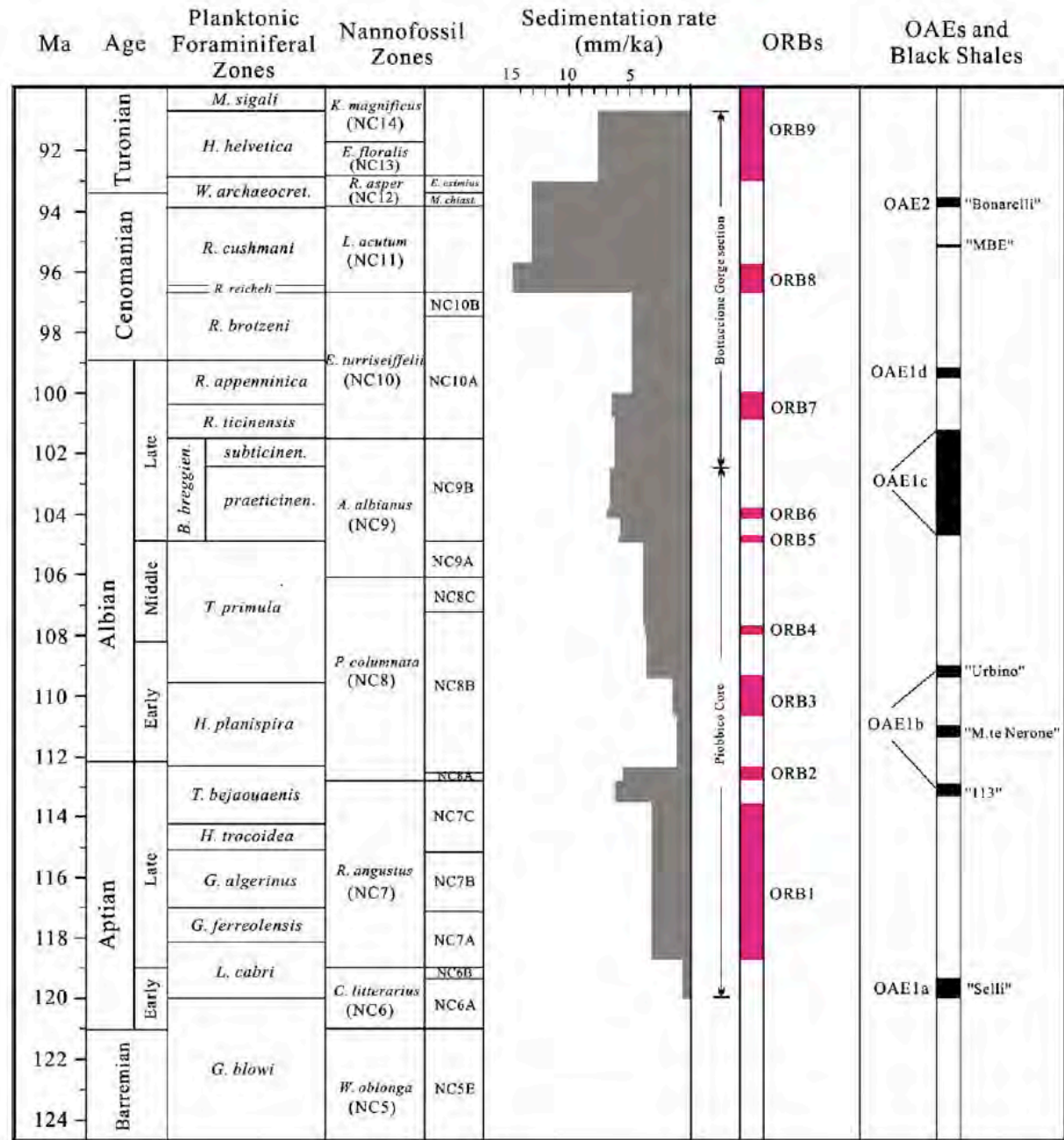


Fig. 9. The schematic summary of upper Barremian to Turonian stratigraphy in the Umbria–Marche Basin, the position of oceanic red beds (ORBs) and ocean anoxic events (OAEs). The mid-Cretaceous integrated calcareous plankton biostratigraphy is after Leckie et al. (2002); sedimentation rates are calculated from combined Piobbico core and the Bottaccione Gorge section.

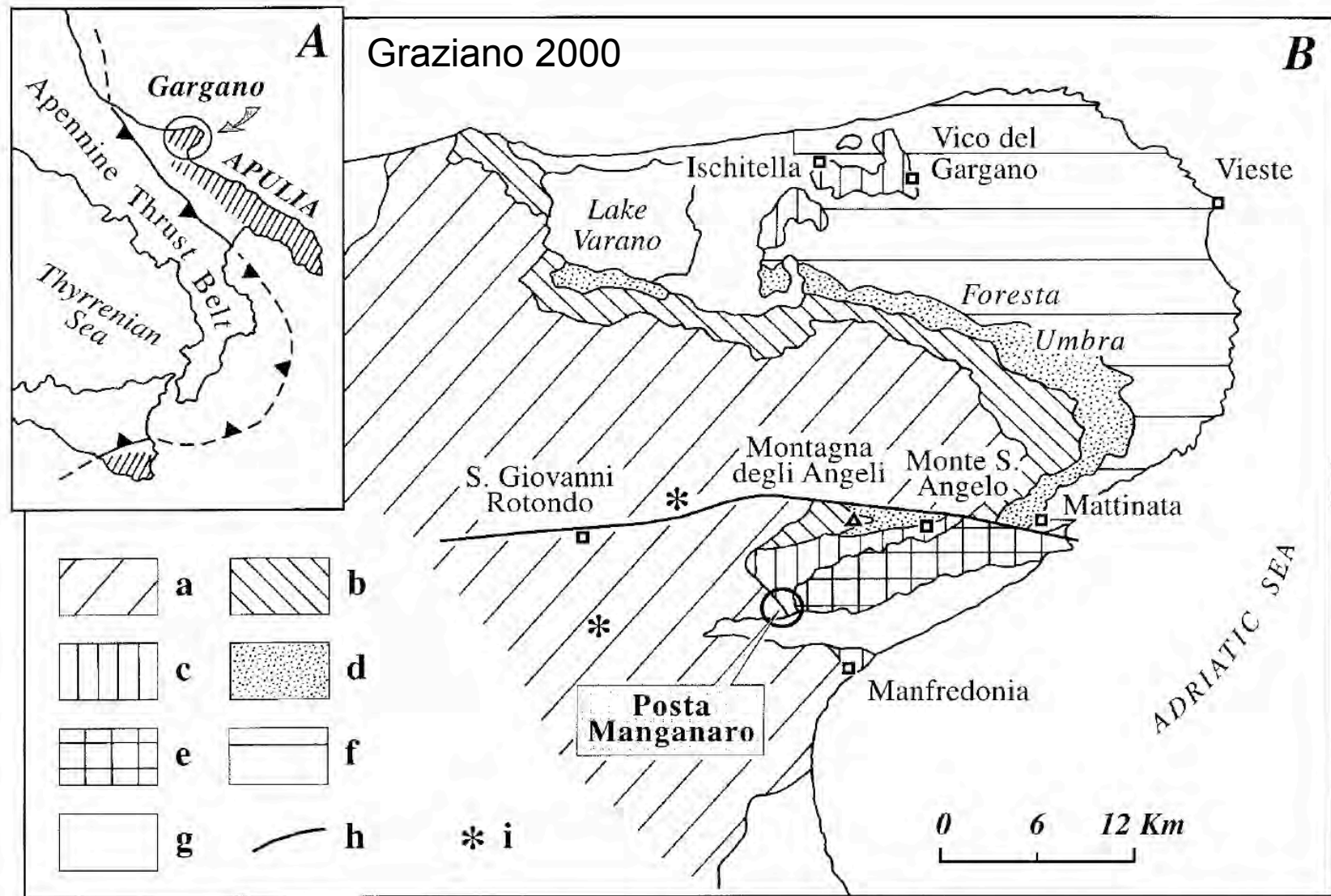


Figure 1. Location of the Apulia foreland in a simplified structural map of Italy (A) and schematic map of the Cretaceous units exposed in the Gargano Promontory (B). The foreland of the Apennine-Sicily thrust belt is indicated by diagonal lines; the solid and dashed line with triangles represents the outer front. a, shallow-water facies associations (Malm–Cenomanian); b, marginal facies associations (Malm–Lower Cretaceous); c, slope and related marginal facies associations (Cenomanian); d, slope facies associations (Tithonian–Albian); e, slope facies associations (Turonian–Senonian); f, basinal facies associations (Berriasian–Senonian *p.p.*); g, continental clastics (Quaternary); h, Mattinata transcurrent fault (late Tertiary); i, main bauxite outcrops (Turonian). The study area of Posta Manganaro is encircled.

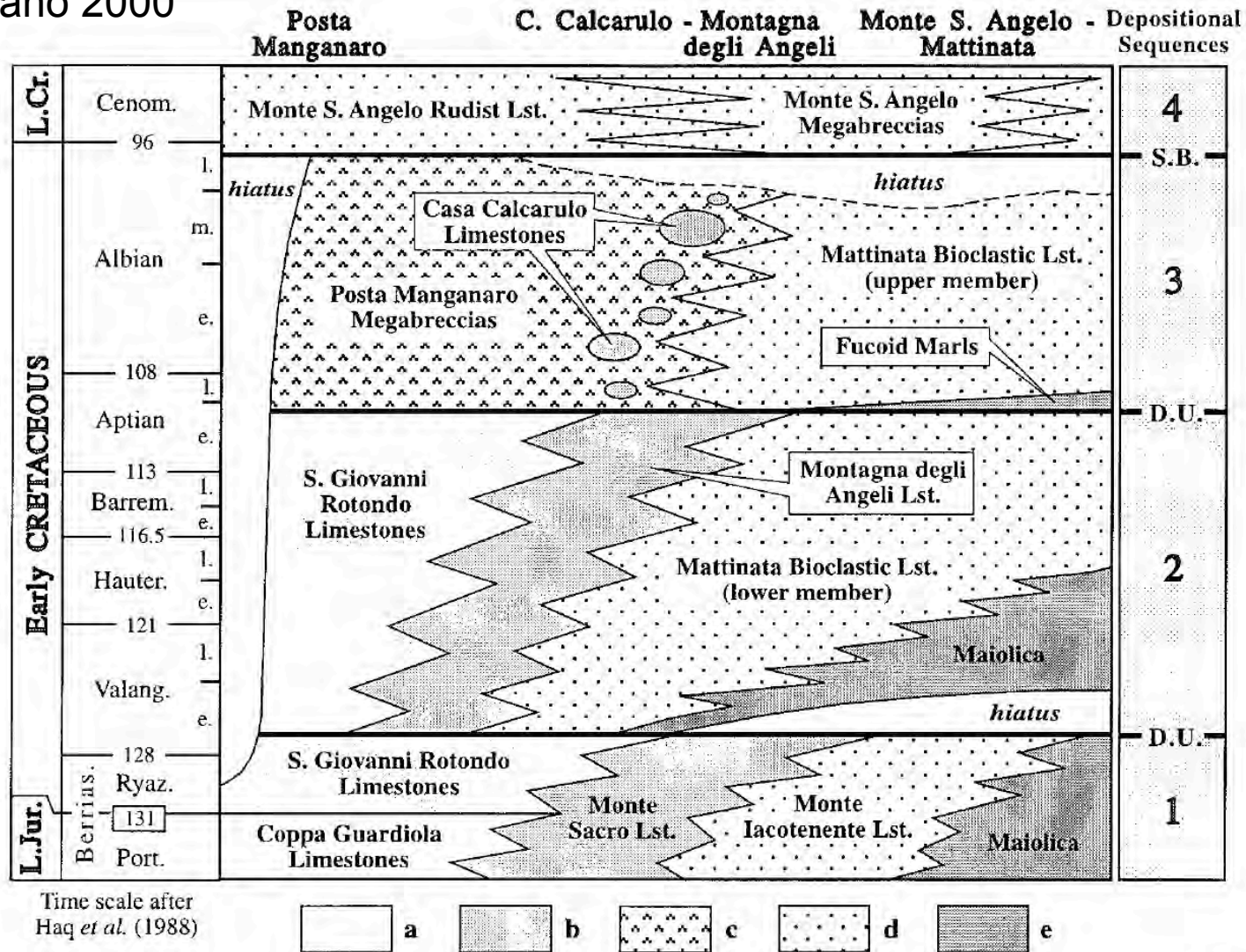


Figure 2. Lithostratigraphic correlation scheme of the Lower Cretaceous formations in the southern Gargano Promontory. The figure represents a roughly west-east oriented platform-to-basin transect. The large-scale stratigraphic architecture results from the articulated stacking pattern of four depositional sequences showing typical transgressive-regressive cycles. Depositional sequences 1 and 2 are bounded by drowning unconformities marking the abrupt retreat of the shallow-water environments (that for the Valanginian is largely based on Bosellini & Morsilli, 1997). 1, Monte Sacro; 2, Monte degli Angeli; 3, Valle Carbonara; 4, Vico del Gargano. S.B., sequence boundary; D.U., drowning unconformity; a, shallow-water successions; b, marginal successions; c, base of slope apron and related successions; d, slope successions; e, basinal successions.

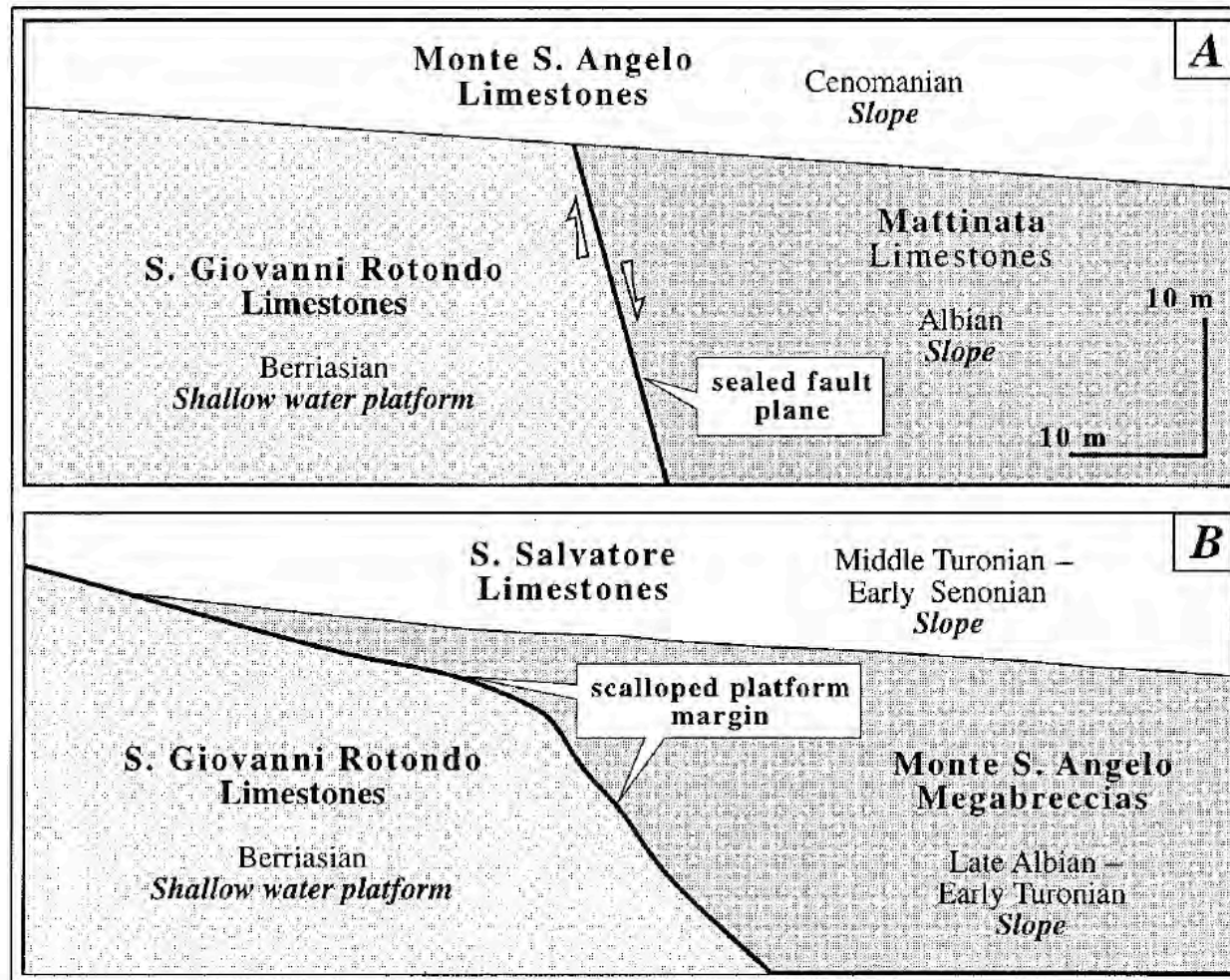


Figure 3. Synthetic diagram taking into account the alternative stratigraphic models proposed for the Cretaceous Apulia Carbonate Platform margin in the southern Gargano Promontory (Posta Manganaro area). A, Early Cretaceous tectonically-induced stratal architecture according to Masse & Borgomano (1987) and Masse & Luperto Sinni (1987) (slightly modified after Masse & Borgomano, 1987). B, Late Cretaceous scalloped configuration of the margin induced by a low stand of relative sea level according to Bosellini (1989), Bosellini *et al.* (1993a, b, 1994), Bosellini & Neri (1993) and Neri (1993) (slightly modified after Bosellini & Neri, 1993).

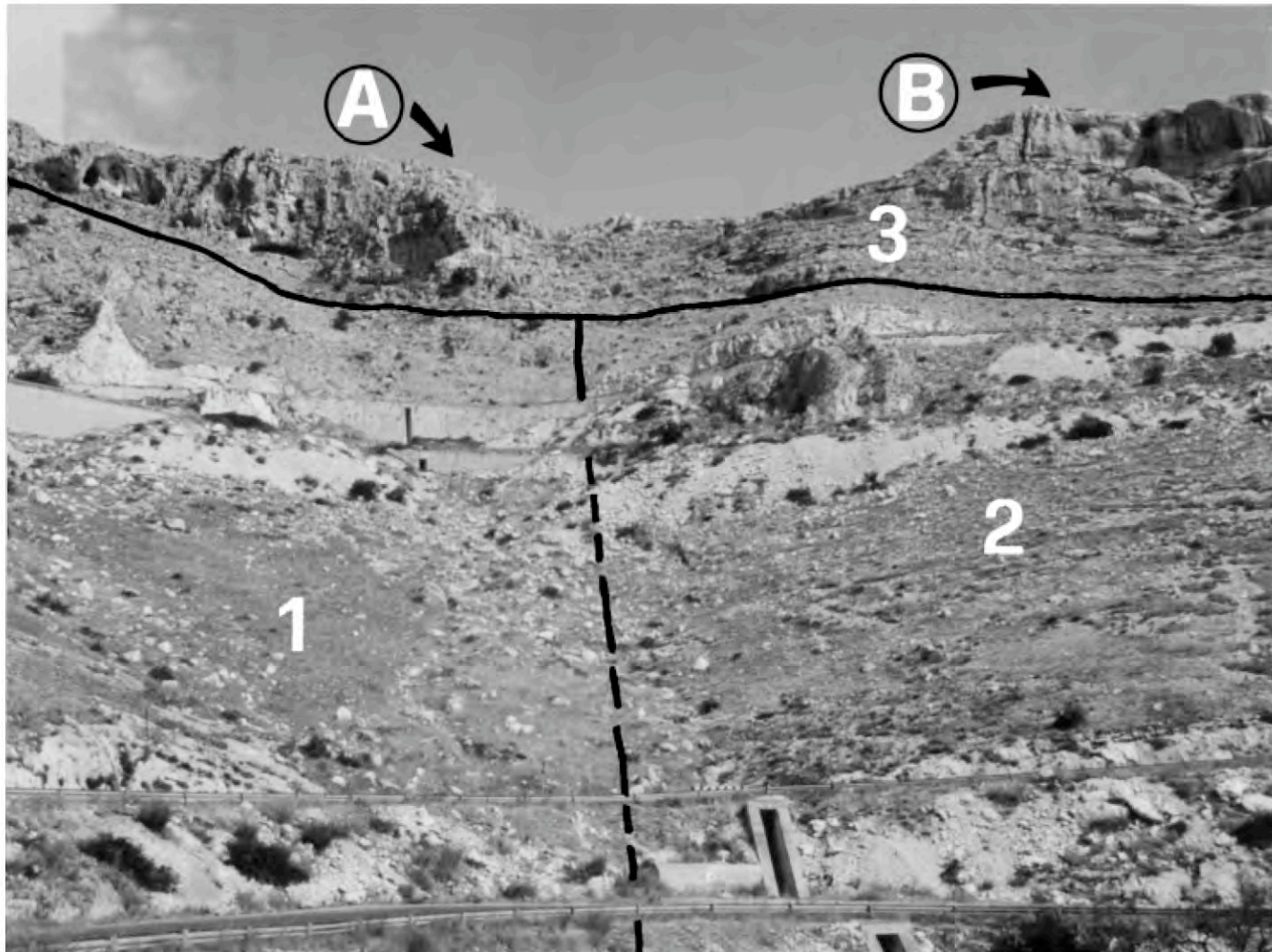


Figure 4. Posta Manganaro stratigraphic architecture exposed along the Ruggiano–Manfredonia road-cut. 1, faintly bedded, tectonized Berriasian shallow-water grainstones and packstones (S. Giovanni Rotondo Limestones); 2, massive, clast-supported mid- to Late Albian megabreccias (Posta Manganaro Megabreccias); 3, Late Albian well-bedded rudist- and *Orbitolina*-rich slope deposits (Monte S. Angelo Rudist Limestones). A, B, locations of the sections sampled; the concealed sub-vertical boundary between units 1 and 2 is indicated by a dashed line.



Figure 4. Posta Manganaro stratigraphic architecture exposed along the Ruggia tectonized Berriasian shallow-water grainstones and packstones (S. G. clast-supported mid- to Late Albian megabreccias (Posta Manganaro Megal and *Orbitolina*-rich slope deposits (Monte S. Angelo Rudist Limestones). concealed sub-vertical boundary between units 1 and 2 is indicated by a c

Graziano 2000

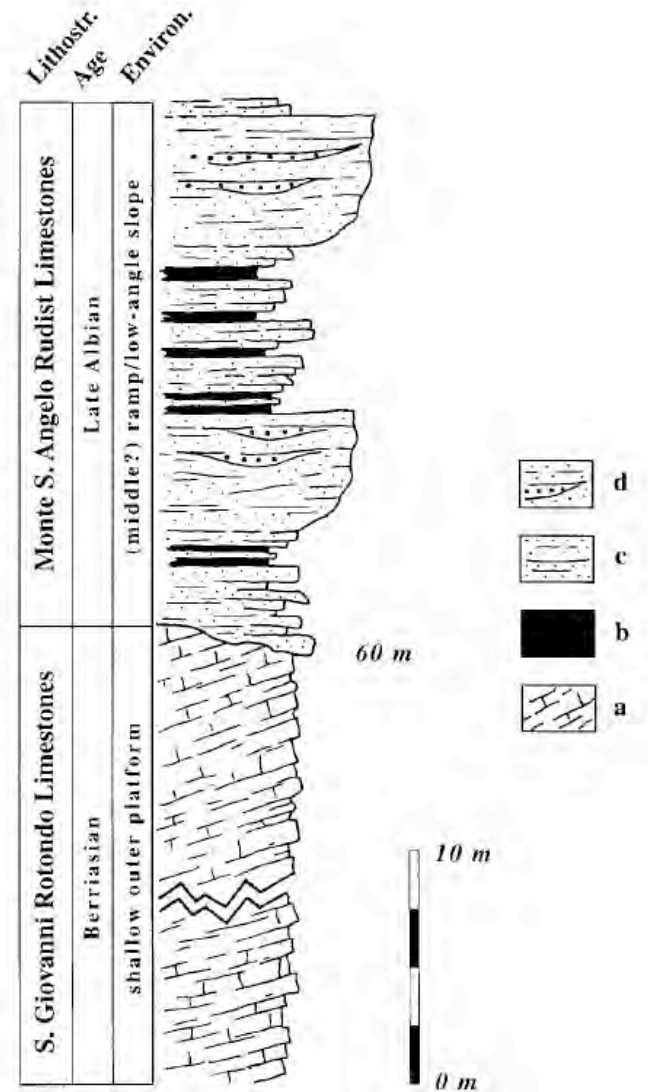


Figure 5. Stratigraphic column of the Lower Cretaceous Apulia marginal succession exposed at Posta Manganaro (section A, Figure 4). The Upper Albian slope bioclastic deposits unconformably overlie the Berriasian tilted carbonate platform. a, oolitic, peloidal and fossiliferous shallow-water grainstones-packstones; b, thin intercalations of laminated pelagic/hemipelagic wackestones and bioclastic packstones; c, fine to coarse bioclastic, turbiditic grainstones; d, coarse bioclastic and intra-bioclastic grainstones-rudstones mainly deposited by sandy debris flows.

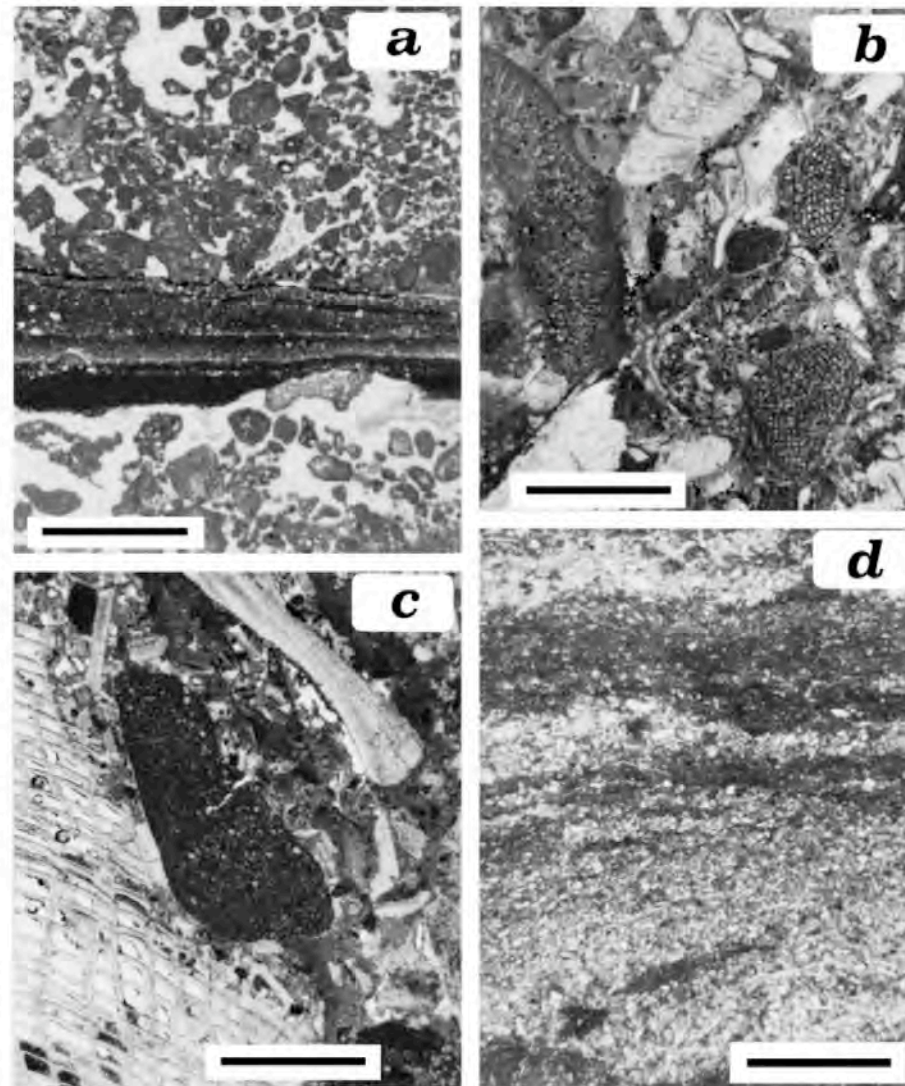


Figure 6. Main microfacies of the Lower Cretaceous carbonate successions (Posta Manganaro). a, peloidal and bioclastic grainstones; a large, early dissolution cavity is filled by vadose silt in thin and graded laminae, Lower S. Giovanni Rotondo Limestones, Berriasian. b, rudist- and *Orbitolina*-rich grainstones, lower Monte S. Angelo Rudist Limestones, *Rotalipora appenninica* Biozone, Late Albian. c, coarse rudist (radiolitid) debris float in a sandy matrix composed of poorly sorted and variously rounded *Orbitolina* and rudist grains, lower Monte S. Angelo Rudist Limestones, *Rotalipora appenninica* Biozone, Late Albian. d, thin, even intercalation of fine bioclastic grainstones interpreted as distal, diluted turbidites and pelagic wackestones bearing scattered planktonic foraminifers (*Rotalipora* sp.), lower Monte S. Angelo Rudist Limestones, *Rotalipora appenninica* Biozone, late Albian. Scale bars represent 2.5 mm.

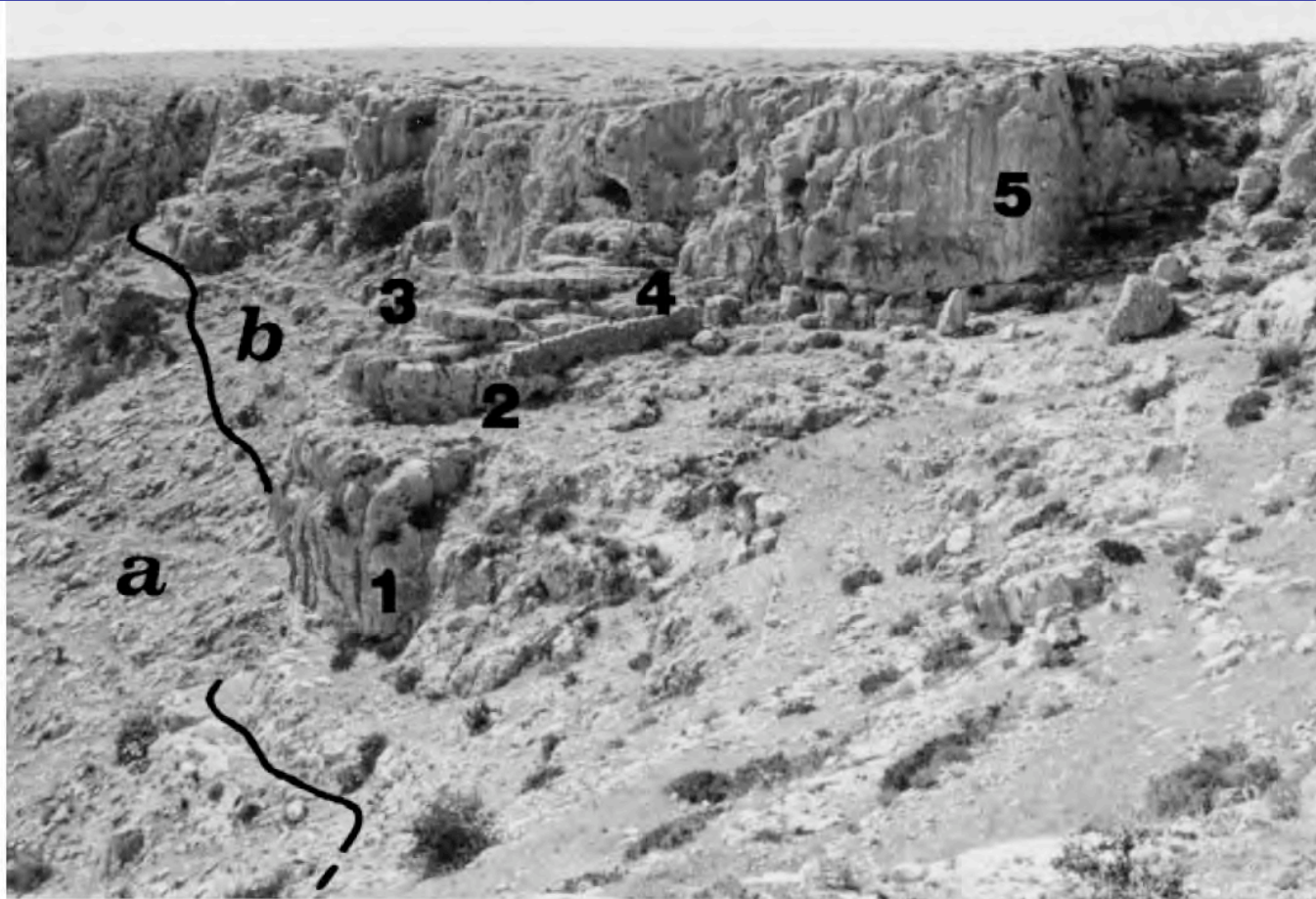


Figure 8. The tilted and eroded Lower S. Giovanni Rotondo Limestones (a) is unconformably overlain (heavy line) by the lower Monte S. Angelo Rudist Limestones (b); the latter unit is organized in five distinct coarsening- and thickening-upward cycles (1–5 in figure) up to some 8 m thick. Cliff edge south of Posta Manganaro.

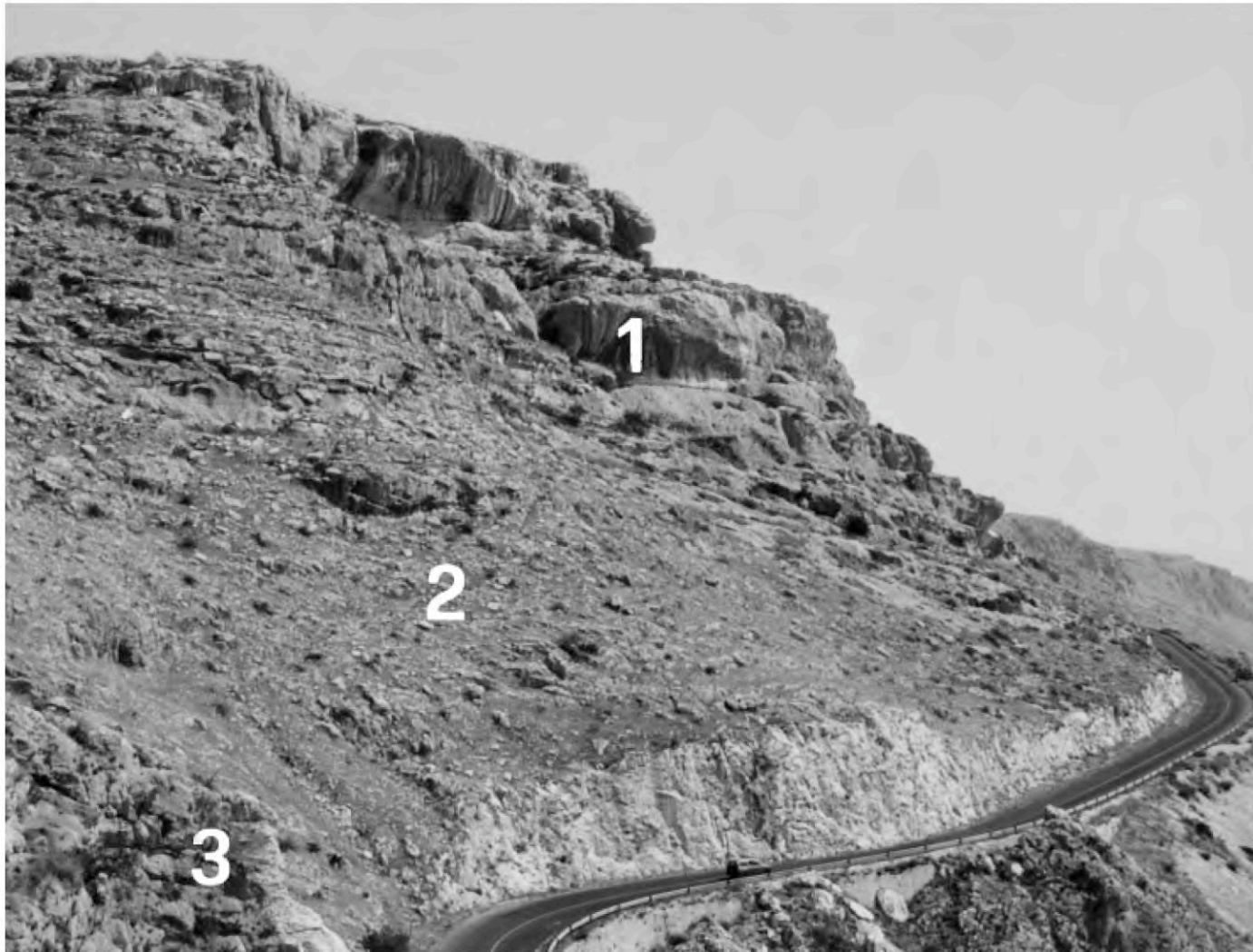


Figure 15. Large-scale, low-angle onlap of the well-bedded lower Monte S. Angelo Rudist Limestones (1) on the upper Posta Manganaro Megabreccias (2); note the distinct coarsening- and thickening-upward cycles within the onlapping deposits. The tectonized S. Giovanni Rotondo Limestones (3) is present in the foreground.

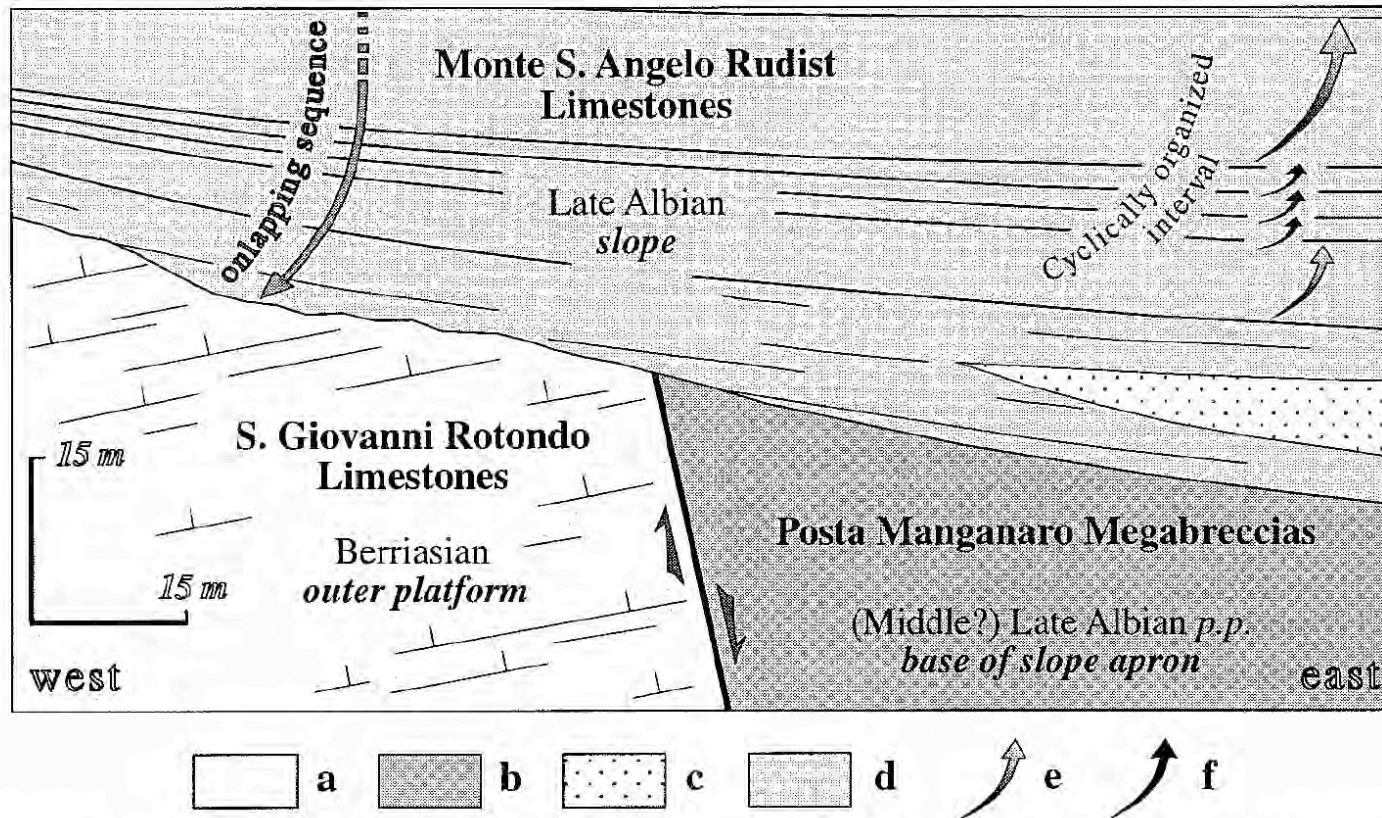
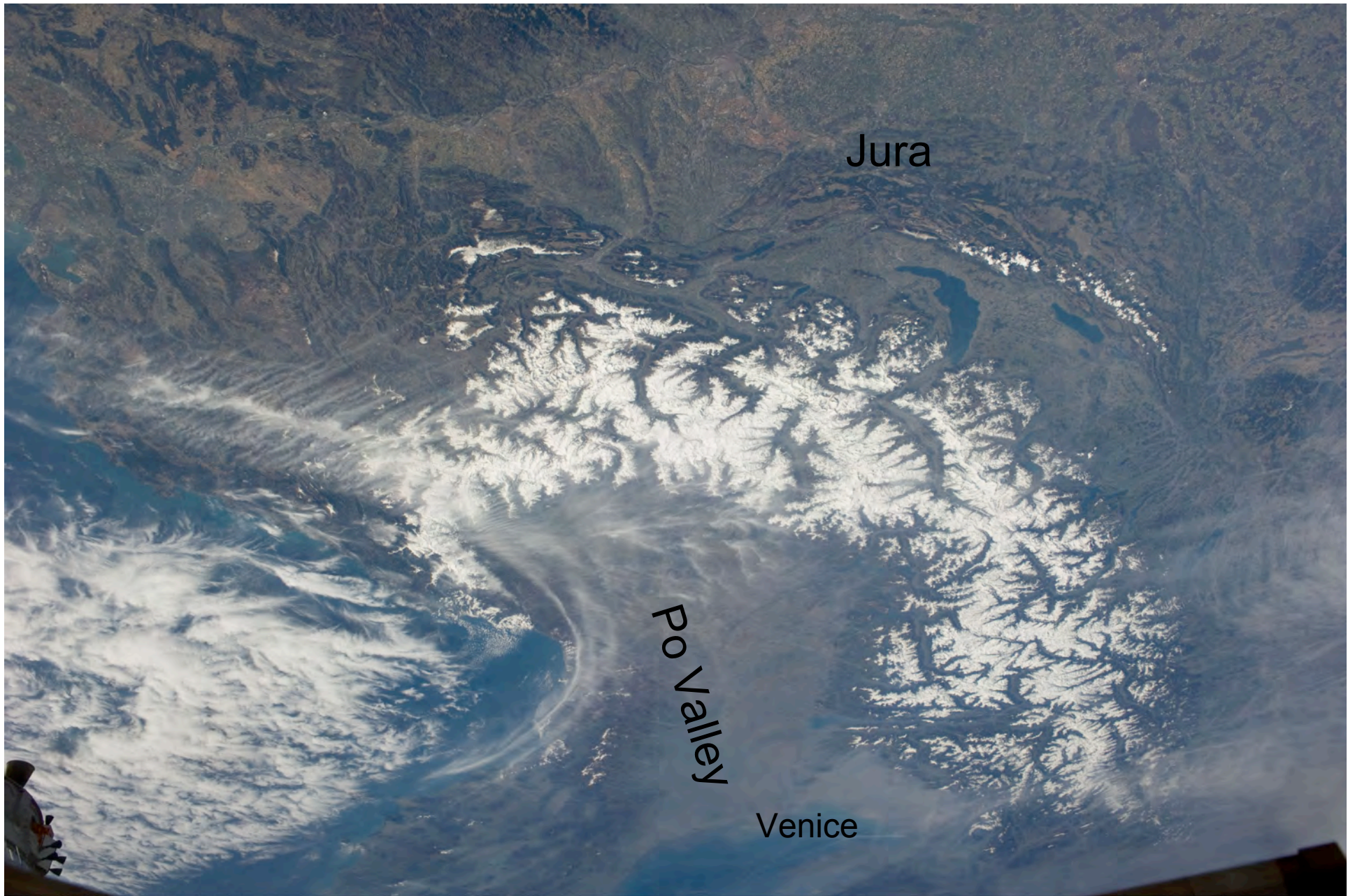


Figure 16. Schematic model of the tectonically-induced stratigraphic architecture at Posta Manganaro (see text for discussion). a, shallow-water oolitic grainstones and bioclastic packstones; b, rock-fall lithic megabreccias without matrix; c, channelized debris-flow megabreccias with rudist-rich bioclastic matrix; d, rudist- and *Orbitolina*-rich bioclastic grainstones-rudstones and hemipelagic wackestones; e, asymmetrical coarsening and thickening upward cycles; f, symmetrical coarsening and thickening upward cycles. Apart from minor differences regarding the stratigraphy of the rudist-rich bioclastic deposits, the model fits well with that proposed by Masse & Borgomano (1987) (see Figure 3a).



ISS027E007723

Alps, Lake Geneva, Adriatic

<http://eol.jsc.nasa.gov/>



The Alps The Dolomites

<http://eol.jsc.nasa.gov/>



Marmalotta Massif from Pardo Pass, Dolomites



Sella Massif and Rosengarten from Gardena Pass, Dolomites



Sella Massif and Pardo Pass, Dolomites



Sella Massif, Dolomites



Sella Massif, Dolomites



Sella Massif, Dolomites



Sella Massif, Dolomites

Darwin's Model of atoll formation by reef growth

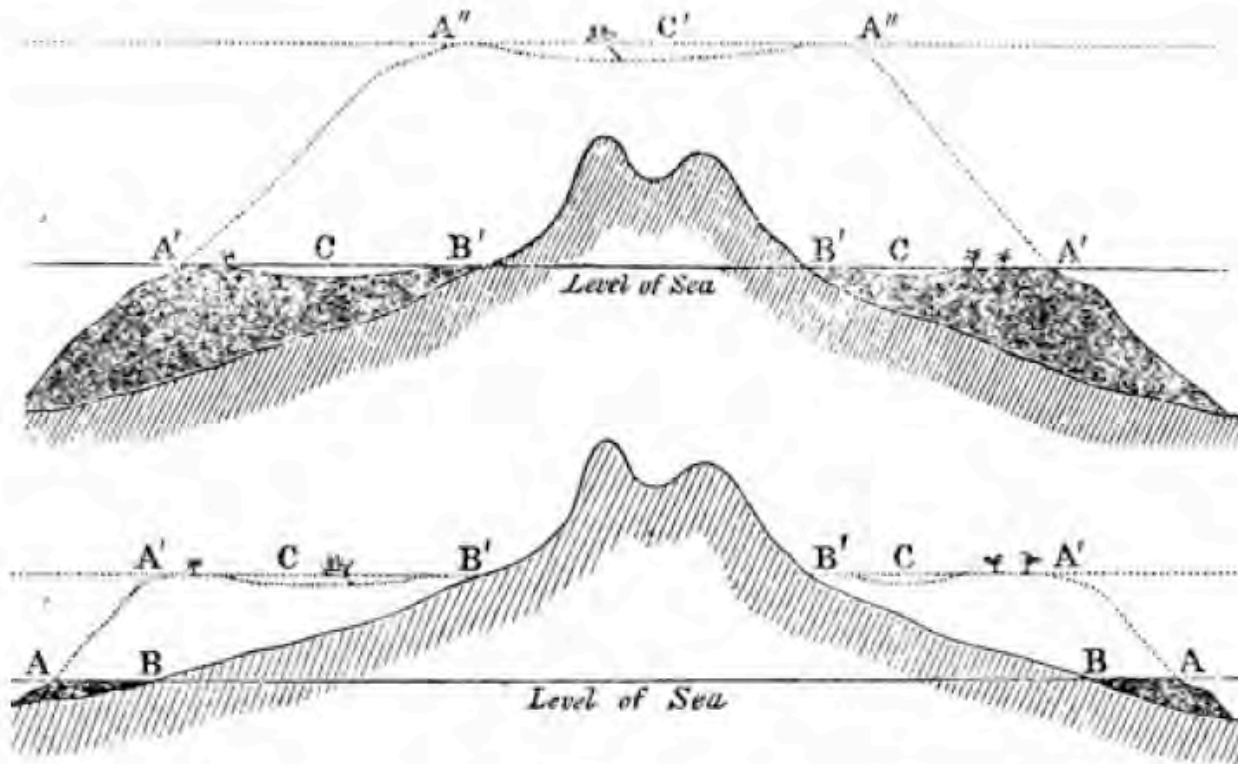


Fig. 1. Model of atoll formation by reef growth (Darwin, 1842). Darwin proposed that volcanic islands with fringing reefs, islands with barrier reefs and atolls (i.e. ring-shaped reefs without a volcanic island) are different stages of one process, governed by subsidence and reef growth. This famous concept is based on surface examination of reefs and comparison of islands and atolls in different stages of development. Data on the slopes and basins were virtually absent at the time.

© 2009 The Authors. Journal compilation © 2009 International Association of Sedimentologists, *Sedimentology*, 56, 191–204

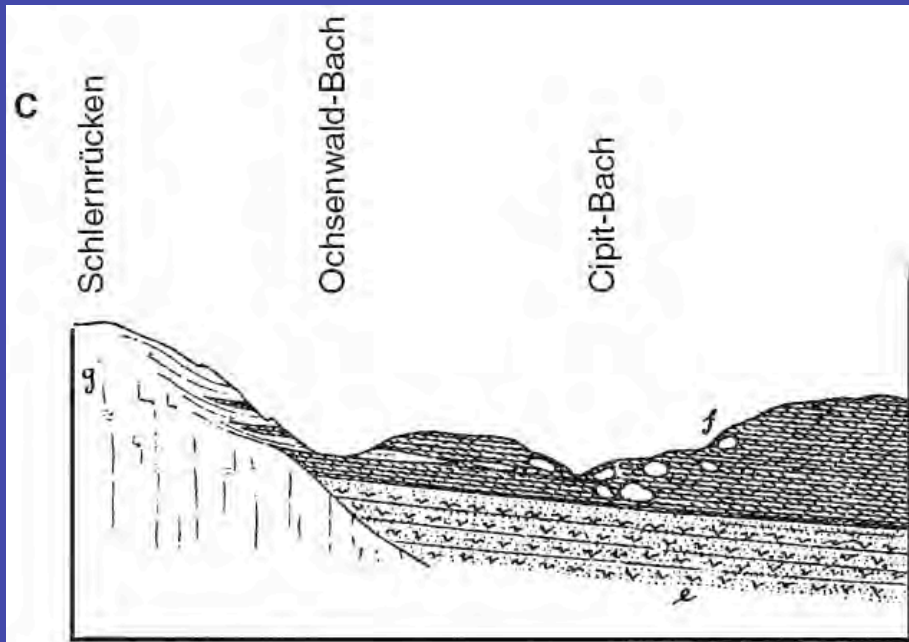
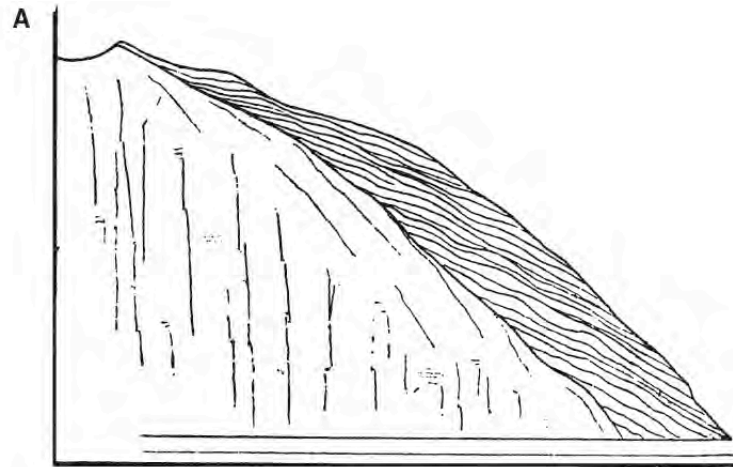


Fig. 2. Examples of slope bedding in the outer parts of the carbonate platforms of the Dolomites (after Mojsisovics, 1879). (A) Scheme of bedding on the flanks of carbonate platforms. (B) and (C) Examples of flank and basin deposits from the Sciliar/Schlern platform. Note the abundant limestone boulders in the basin sediments.

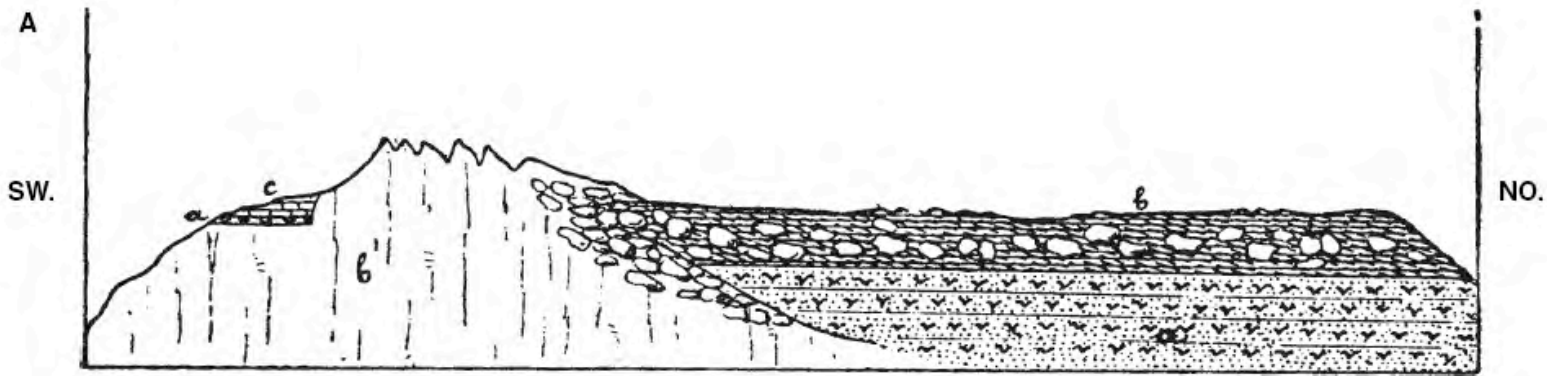


Fig. 3. Boulders of reef material at platform–basin transition. (A) Cross-section based on outcrop observations, showing boulders of reef material in basin sediments (after Mojsisovics, 1879). Mojsisovics interpreted the boulders (called Cipit blocks) as reef fragments that had slid down the slope; Richthofen (1860) viewed most of them as erosional remnants of limestone beds intercalated in marly basin sediments. Recent studies confirm the interpretation of Mojsisovics for many boulders. However, some boulders are erosional remnants of debris flow breccias where microbial framebuilders continued to grow on the unburied parts of the boulders (Brandner *et al.*, 1991). Thus, the interpretation of Richthofen, too, was confirmed partly. (B) Photograph of cliniform tongue disintegrating into boulders as it thins out in argillaceous basin sediments. Grey rockface under letter (B) is about 50 m high. Sella Mountain, south slope (L. Keim photograph, image flipped to match (A)).



Fig. 4. Interfingering of shallow-water carbonate deposits and argillaceous basin deposits in the Dolomites (after Mojsisovics, 1879). Outcrop shows bodies of massive dolomite (interpreted as coral reefs by Mojsisovics) wedging out in deeper-water shales and marls. High cliffs at the back represent platform carbonates with, originally horizontal, topset bedding in the uppermost parts. Symbols: CM = basin deposits; CDo = platform and slope carbonates (nearly all dolomite); CDo₁₋₃ = individual tongues of platform and slope carbonates (contact CDo₂/CDo₃ is overprinted by local thrusting during Alpine deformation). Tongues CDo₁₋₃ are often referred to as 'Richthofen Reef'.

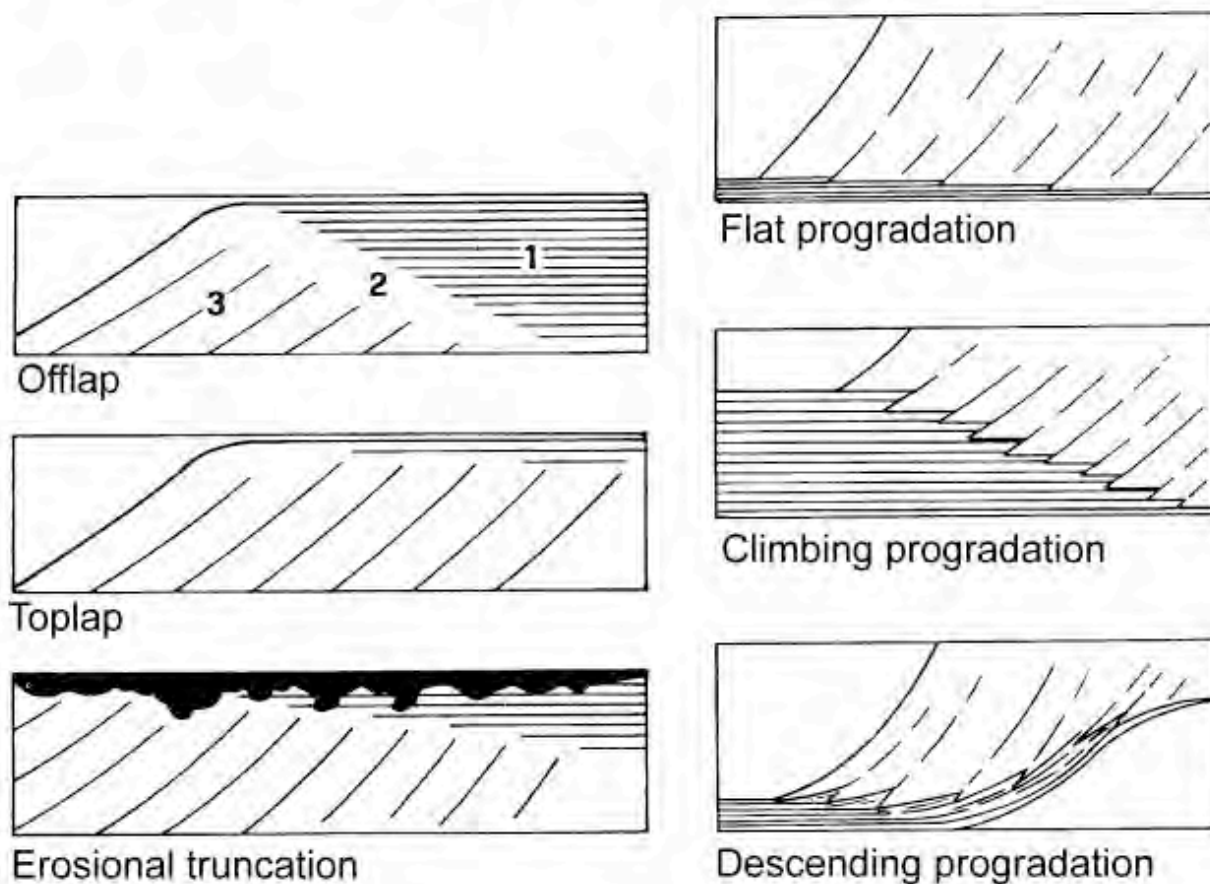


Fig. 5. Lap-out patterns, defined originally for use in seismic interpretation, observed in outcrops of the Dolomites. Left: toplap; right: downlap. After Bosellini (1984).



Fig. 6. Interfingering of platform slope and basin facies on the NW flank of Picco di Vallandro/Dürrenstein. Sand and rubble of the lower slope is now present as tongues of clean dolomite and limestone that wedge out in argillaceous limestones and marls of the basin. Argillaceous basin sediments wedge out in an upslope direction. Slope tongues range from <1 m to over 100 m in thickness. (A) Overview of the mountain flank showing the thickest tongues. Platform lies to the left, basin to the right; structural dip exaggerates the depositional dip of the slope. Highest peak rises about 1100 m above scree slopes in the lower right corner of photograph. Arrows indicate the location of (B). (B) Twenty metre thick tongue of slope breccia wedging out in basin sediments.



Fig. 8. Parallel bedding of the platform interior of the Triassic Latemar atoll. Hierarchy of bedding rhythms is apparent. Continuous outcrops allowed tracing of beds and groups of beds across the platform (Egenhoff *et al.*, 1999; Zühlke *et al.*, 2003). Interpretation and dating of these beds led to the Latemar debate (see Fig. 9). Thickness of platform deposits shown in photograph is about 700 m.

<i>Berger & Loutre 1994 cycle periods from celestial mechanics</i>			<i>P</i> 18 21	<i>O</i> 36 45	<i>E₁</i> 100	<i>E₂</i> 400?
Zuehlke <i>et al.</i> 2003	4-2	14-16	18-22	36-48	95-106	270-617
Preto <i>et al.</i> 2001	18-22	36	99		400	
<i>Berger & Loutre 1994 cycle periods from celestial mechanics</i>	18 21 <i>P</i>	36 45 <i>O</i>	100 <i>E₁</i>		400 <i>E₂</i>	

Fig. 9. Latemar debate in summary. Bold text: contrasting orbital interpretations of platform bedding by Zühlke *et al.* (2003) and Preto *et al.* (2001, 2004). Plain text: Periods of orbital parameters estimated by Berger & Loutre (1994); P = precession, O = obliquity, E₁ = eccentricity peaks around 100 kyr, E₂ = eccentricity peaks around 400 kyr. The two interpretations differ by a factor four in time. Zircon geochronology (Mundil *et al.*, 2003), magnetic stratigraphy (Kent *et al.*, 2004) and ammonite stratigraphy (Brack *et al.*, 1996) are best compatible with the interpretation of

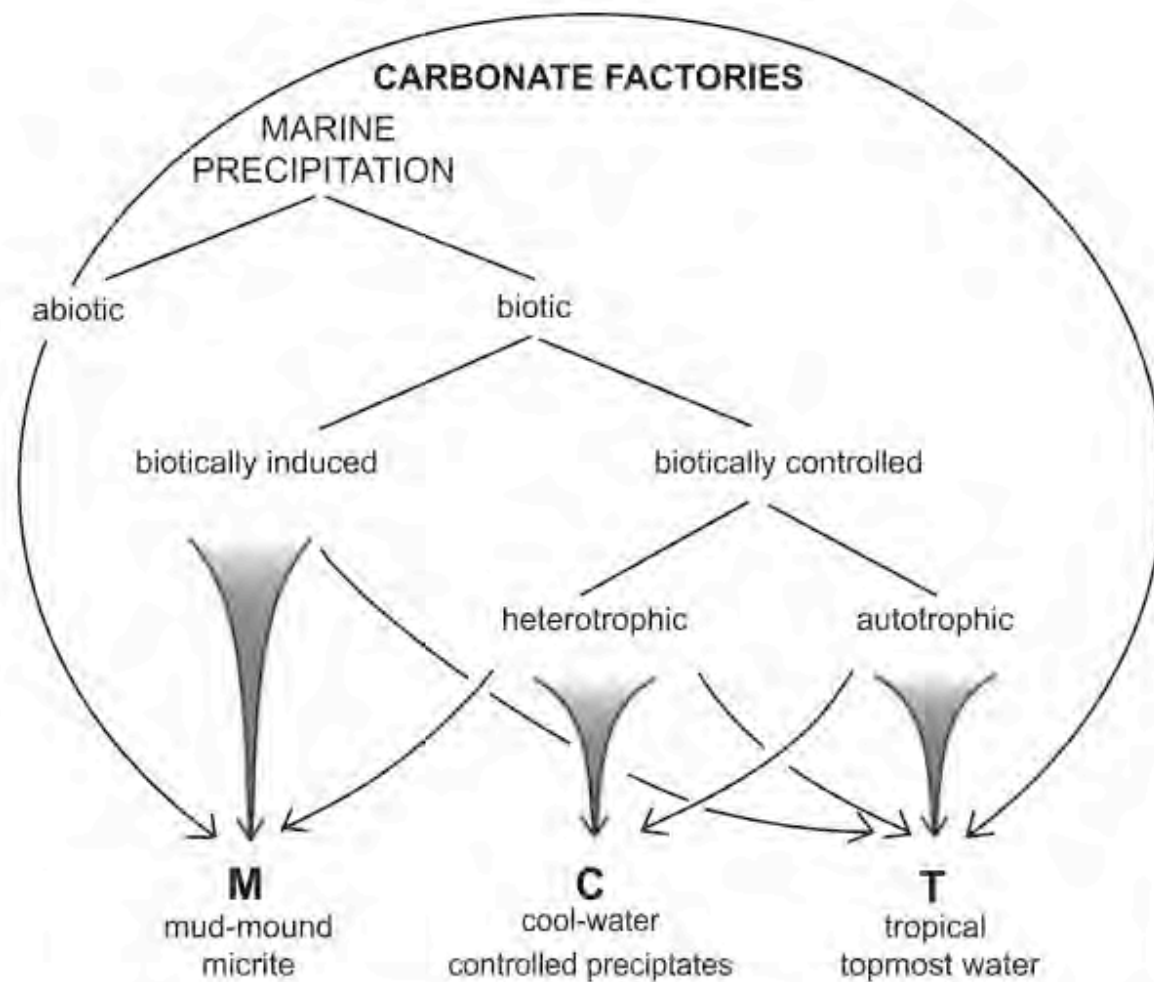


Fig. 10. Basic modes of marine carbonate precipitation and their combination into three carbonate production systems or 'factories' (after Lowenstam & Weiner, 1989; Schlager, 2005).

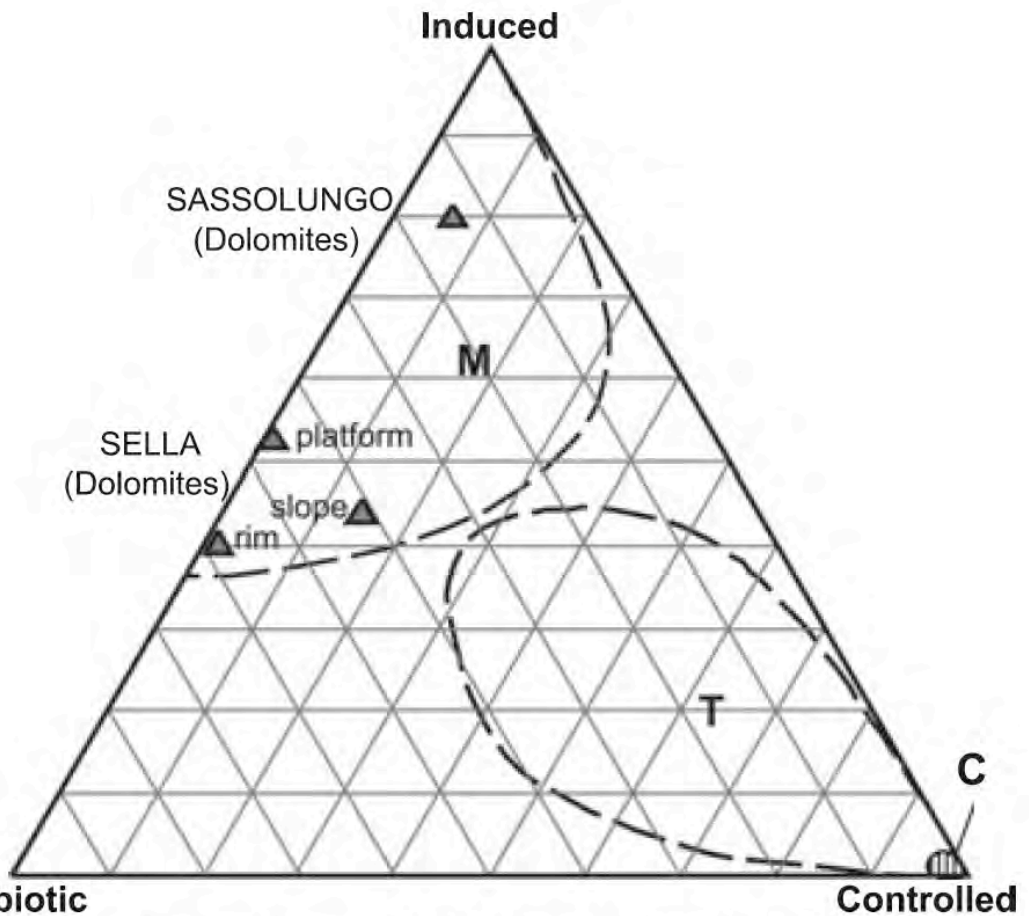


Fig. 12. Proportions of abiotic, biotically induced and biotically controlled precipitates in well-documented carbonate formations. The T factory and M factory are separate, C factory clusters tightly in the biotically controlled corner. According to the coral-reef interpretation, Triassic carbonates of the Dolomites should plot in the field of the T factory, but the quantitative data from Sasso Lungo and Sella fall clearly in the field of the M factory. Based on Russo *et al.* (1997), Keim & Schlager (2001) and Schlager (2003).